The effect of different cements and pozzolans on chloride ingress into concrete

Johannesson, Björn

2000

LUND INSTITUTE OF TECHNOLOGY
LUND UNIVERSITY

Division of Building Materials

The Effect of Different Cements and Pozzolans on Chloride Ingress into Concrete

Björn Johannesson

TVBM-3093 Lund 2000

LUND INSTITUTE OF TECHNOLOGY
LUND UNIVERSITY

Division of Building Materials

The Effect of Different Cements and Pozzolans on Chloride Ingress into Concrete

Björn Johannesson

TVBM-3093 Lund 2000

ISRN LUTVDG/TVBM--00/3093--SE(1-62)
ISSN 0348-7911 TVBM

Lund Institute of Technology
Division of Building Materials
Box 118
SE-221 00 Lund, Sweden

Telephone: 46-46-2227415
Telefax: 46-46-2224427
www.byggnadsmaterial.lth.se

The Effect of Different Cements and Pozzolans on Chloride Ingress into Concrete

Björn F. Johannesson
Lund Institute of Technology, Division of Building Materials
Box 118, SE-221 00 Lund, Sweden

Abstract

Chloride profiles were measured on ten different concrete qualities. The effect of two different cements, an ordinary Portland cement, OPC, and a sulfate-resistent Portland cement, SRPC, with and without inclusion of silica fume and fly ash was investigated. The samples were exposed to a 3 wt% sodium chloride solution for 119 days. Two different preparations before exposure were studied. Both types of preparations consisted of one-day membrane hardening after casting. After this a set of samples were dried for two weeks and then rewetted in tap water for one week before exposure. The other set of samples were stored in tap water one week before exposure to chlorides. The chloride content profile in concrete was measured by removing approximately 1.2 mm thick layers, from the exposed surface, by grinding. The concrete powder, collected from different depths from the surface, was dissolved in an acid and analyzed for chlorides by an ion-selective electrode. The obtained chloride profiles were evaluated in two ways. The first consisted of a simple curve fitting to the solution to Fick's second law, without any special attention to boundary conditions, in order to obtain the so-called effective diffusion constant. The other method of evaluating the measured values consisted of a more detailed hypothesis accounting for dielectrical effects, diffusion of free ions in pore solution, and chemical reaction such as binding of chlorides and dissolution of hydroxide from solid hydration products. Both methods of evaluating the measured data gave the result that the OPC concretes resisted chloride ingress better than SRCP concretes at the same water to binder ratios when stored in water before exposure.

The OPC concrete in which 5% of the cement content were replaced by silica fume resisted chloride ingress significantly better than the SRPC with the same relative amount of silica fume. This behavior was independent of curing conditions.

1 Introduction

The magnitude of chloride ingress is investigated for a case where a part of the cement content is replaced by pozzolans. The cements used are a Swedish ordinary Portland cement, OPC, trademark 'Slite Std', and a low-heat sulfate-resistent Portland cement, SRPC, trademarked 'anläggningscement'. The pozzolans tested are silica fume and fly ash. Ten different types of concretes are used in the investigation. Three concretes are based on the SRPC, one is based on cement without any pozzolan and the other two contain either 5% silica fume or 5% silica fume together with 20% fly ash, replacing cement. These samples were manufactured at the water to binder ratios 0.40 and 0.55, which constitute in total six samples based on SRPC. The OPC concretes used are two samples with the water to binder ratios 0.40 and 0.55 with no pozzolans and two samples with the water to binder ratios 0.40 and 0.55 containing 5% silica fume replacing cement.

All samples were membrane-hardened for one day after casting. After this the sealing was removed and the samples were allowed to dry in room climate for two weeks. An estimation of the active porosity was achieved by letting some of the samples suck water until no weight gain could be registered any longer. The total volume concentration occupied by the capillary sucked water, i.e. the active porosity, is used as an important material property when evaluating the measured data in terms of properties such as free diffusing ions in pore solution and the amount of bound ions.

The results in terms of chloride ingress in the samples dried before exposure are compared to a set of samples stored for one week in tap water before exposure to chlorides. These last set of samples were never dried before exposure to chlorides. The total porosity was, therefore, calculated using a formula including the hydration degree, water to binder ratio and the cement content in the concrete mix. The degree of hydration at the time of chloride exposure was measured for all different concrete types tested.

Two types of methods of evaluating the measured results in terms of chloride profiles are used. The most direct approach consists of fitting the

solution to Fick's second law to the measured data in order to obtain the so-called effective diffusion constant. In this method no special attention is paid to the applied boundary condition in the experiment. The outermost measured concentrations (in the range of 0-5 mm from the exposed surface) is, furthermore, ignored since these values, in general, deviate very much from the shape of the fitting curve in use. The second approach to evaluate the measured data consists of treating diffusion, chemical binding and leaching of several different ions appearing in pore solution or as solid components. The key issue in this approach is to define an active water-filled porosity in which volume the dissolved ions are present. The diffusion velocities are constituted in a way that the total electron valence among the positively and negatively charged ions always is very close to zero at every material point and at every time level.

The diffusion and ion mobility constants for ions in bulk water are used together with a tortuosity factor taking into account the porosity and the shape of the pore system. This scaling factor is found to be in the range of 0.004-0.010 for the examined concretes. In [1] the tortuosity factor is measured on concrete using a gas diffusion technique. The values obtained for water to binder ratios 0.40 and 0.55 are in the range 0.007-0.020, which agrees well with the values found in this study. Theoretical considerations of tortuosity effects on Portland cement paste can be studied in, e.g. [2], where percolation theory is used. It is found that the tortuosity factor is a continuous function of the saturation degree until a breakpoint is reached which corresponds to the liquid water becoming unconnected, i.e. when the wetting phase does not percolate. Yet another theoretically based study concerning tortuosity can be found in [3], dealing with diffusion of ions in cement-based materials using a homogenization technique in connection with a continuum mechanical concept.

The dissolution and binding reactions considered are binding of chlorides by ion exchange with solid calcium hydroxide present in the hydration products, dissolution of ions from the solid calcium hydroxide, into the pore solution, and dissolution of already formed solid calcium chloride. Both equilibrium conditions and reaction kinetics are constituted for these reactions. Binding isotherms for chlorides, i.e. the equilibrium conditions between the concentration of chloride ions in pore solution and ions being physically or chemically bound into the solid micro-structure are extensively studied in the literature, e.g. see [4] and [5]. Measurements on the kinetics of chloride binding can further be found in [6].

A more detailed method for establishing a model, from which the experimental data are to be evaluated, has a number of benefits compared to the simple method of using the effective diffusion constant concept. The most important issue is that physically correct boundary conditions are used, i.e., in this case, the concentrations of ions in the solution to which the samples are exposed. Another good property of the method is that once the tortuosity factor has been determined, all the diffusion constants and ion mobility constants, for the considered ions in pore solution, can be scaled with the same number. This is due to an assumption stating that all ions dissolved in pore solution are affected by the porosity and shape of the pore system in an identical manner. The approach becomes possible and significant since diffusion of dissolved ions in water-filled porosity and chemical effects among dissolved ions in pore solution and solid constituents, such as binding and leaching, are treated by separate constitutive assumptions.

The solution of the proposed set of coupled equations for the different dissolved ions and solid constituents gave one possible explanation for the experimentally verified phenomenon of having a maximum chloride content at approximately 2-4 mm from the exposed surface as shown in the section 4. This phenomenon is most dominant for samples dried before exposure to a constant outer chloride solution or samples having high water to binder ratios, never being dried before exposure. In [7] the same phenomenon has been reported, i.e. a maximum in either chloride, sodium or both elements was found a few millimeters below the exposed surface. This phenomenon was, further, observed to be most dominant in samples air cured before exposure to a chloride solution spray.

Different numerical simulation runs revealed that the cause of this behavior can be a combined effect of electrically driven diffusion among positive and negative ions in pore solution and the fact that calcium ions (and hydroxide ions) are dissolved from the solid calcium hydroxide in the hydration products. Loosely speaking, the chloride ions take part in the process of achieving equality of negative and positive charges in pore solution, and the main reason for the momentary imbalance is the time scale for leaching of the calcium and hydroxide ions, previously appearing as solid components, and the time scale for the same ions reaching the surrounding storage solution by diffusion.

The tortuosity factor for scaling concentration and electro-potential gradient-driven diffusion was found to be correlated to the porosity of the samples having the same cement and pozzolan composition but different water to binder

ratios. No general dependency on porosity was found, however, among the different mixes using different cements and pozzolans. This is presumably due to different cements and pozzolans creating not only different porosities but also significantly different shape of the pore systems available for water and dissolved ions. This is in accordance with the conclusions drawn in [8], where it is observed that pastes containing OPC with 30% fly ash are substantially more porous than plain OPC pastes, of the same water to cement ratio, yet the effective diffusivity determined for the blended paste has a value approximately one-third that of the OPC paste.

The binding capacity for chlorides was found to be correlated to the mass density concentration of cement in the concrete mix when comparing concrete with the same cement and pozzolan composition but at different water to binder ratios, i.e. the same conclusion as compared to the correlation of the tortuosity factor. The differences obtained when comparing the general dependence of binding capacity of chlorides to the mass density concentration of binder in mix is, again, believed to be a consequence of different properties, such as specific surface, depending on the combination of cement type and pozzolans. The concentration of bound chloride is found to increase with increased water to binder ratio and cement content. The chloride binding was observed to increase by a factor of 3 when decreasing the water to binder ratio from 0.55 to 0.40. Furthermore, the replacement of cement content by 5 wt.% silica fume reduced the binding by a factor of 2 when compared to plain OPC concrete and a factor of 3 when replacing SRPC with 5% silica fume. The same type of behavior has been found in [9].

Both the methods studied leading to the effective diffusion constant and the method of considering interaction among different ions, gave the result that OPC concrete with 5% silica fume replacing cement, has the best ability to resist chloride ingress of all the examined concrete qualities in this study. This result was independent of the two different examined curing conditions. The concrete with pure SRPC was further found to resists chloride ingress at the same level as SRPC with 5% silica fume and 20% fly ash replacing cement, when using the evaluation method of considering interaction among different ions. The effective diffusion constant method, however, gave the result that SRPC concrete with 5% silica fume and 20% fly ash replacing cement is significantly more resistant to chloride ingress than concrete mixes based on pure SRPC. The important different results obtained, depending on the evaluation method used, is mainly due to ignoring measured data near the exposed surface when using the effective diffusion constant concept and

also due to ignoring dielectical effects in the simpler method.

The effect of different cements and pozzolans on chloride ingress into cement paste and concrete has been extensively studied using different methods, e.g. see [10], [11], [12], [13] and [14].

2 Experimental Procedure

The most common types of studies concerning chloride ingress into cement-based materials are long-term field measurements, accelerated laboratory tests using an external applied electrical field and long-term immersion tests in controlled conditions in the laboratory. The exposed specimens are usually analyzed for chlorides by collecting concrete powder in layers from the exposed surface; this powder is usually analyzed with a chloride ion-selective electrode or by using titration. In the so-called steady state methods chloride concentration profiles in the material are not measured but rather evaluated by measuring the steady state flow of chloride ions through samples. Different types of measurement techniques can be studied in, for example, [15] and [16].

The experiments in this study include evaluation of the total chloride profiles, i.e. bound and free chlorides, for 14 different concrete samples stored in a 3 wt.% sodium chloride solution for 119 days. The mix proportions of the concrete are shown in Tables 1-10. Two different preparations, before exposure to chlorides, were studied in order to check its influence on chloride penetration, for the different cements and pozzolans used in the concretes. The hydration degree was measured at the time of chloride exposure. These tests were performed on parallel samples exposed to the same pre-conditioning as the samples exposed to chlorides. The hydration tests were performed in order to obtain a quantitative measure of the total porosity.

The compressive strength was measured on two samples of each studied concrete quality after 1 week's hardening. The active porosity was estimated, for the concrete qualities dried before exposure, by letting 25 mm thick dried concrete discs suck water until equilibrium was reached. The total weight gain due to capillary suction, at equilibrium, serves as a quantitative measure of the active porosity for a given sample volume.

The concrete was cast in PVC cylinders having the inner diameter 100 mm and the length 180 mm. The samples were vibrated for approximately one minute before being sealed with plastic bags. After one day's hardening

Table 1: Mix proportions, SRPC concrete, water to cement ratio 0.40, slump 30 mm.

	Mass density (kg/m^3)	Weight in mix (kg)	Moisture (kg)
Cement (SRPC)	420	9.66	-
Silica	-	-	-
Fly ash	-	-	-
Aggregate 0-8 mm	939	21.68	0.0825
Aggregate 8-12 mm	867	19.94	-
Water	168	3.6873	-
Plasticizer	6.30	0.1449	0.09418

Table 2: Mix proportions, SRPC concrete, water to cement ratio 0.55, slump 25 mm.

	Mass density (kg/m^3)	Weight in mix (kg)	Moisture (kg)
Cement (SRPC)	340	7.48	-
Silica	-	-	-
Fly ash	-	-	-
Aggregate 0-8 mm	971	21.44	0.0769
Aggregate 8-12 mm	861	18.94	-
Water	187	4.0371	-
Plasticizer	-	-	-

Table 3: Mix proportions, SRPC concrete, 5 percent silica, water to binder ratio 0.40, slump 50 mm.

	Mass density (kg/m^3)	Weight in mix (kg)	Moisture (kg)
Cement (SRPC)	399	8.78	-
Silica	21	0.462	-
Fly ash	-	-	-
Aggregate 0-8 mm	898	19.84	0.0790
Aggregate 8-12 mm	889	19.76	-
Water	168	3.5269	-
Plasticizer	6.30	0.1386	0.0901

Table 4: Mix proportions, SRPC concrete, 5 percent silica, water to binder ratio 0.55, slump 35 mm.

	Mass density (kg/m^3)	Weight in mix (kg)	Moisture (kg)
Cement (SRPC)	323	7.11	-
Silica	17	0.374	-
Fly ash	-	-	-
Aggregate 0-8 mm	966	21.33	0.0808
Aggregate 8-12 mm	857	18.85	-
Water	187	4.0332	-
Plasticizer	-	-	-

Table 5: Mix proportions, SRPC concrete, 5 percent silica, 20 percent fly ash, water to binder ratio 0.40, slump 50 mm.

	Mass density (kg/m^3)	Actual weight (kg)	Moisture (kg)
Cement (SRPC)	315	6.93	-
Silica	21	0.462	-
Fly ash	84	1.848	-
Aggregate 0-8 mm	845	18.68	0.09295
Aggregate 8-12 mm	916	20.15	-
Water	168	3.5429	-
Plasticizer	4.20	0.0924	0.0924

the samples were cut into three discs, two of them with a thickness of 25 mm and one with a thickness of 60 mm. The 60 mm sample, to be used in the chloride exposure test, was sealed with silicon in the joint between PVC and concrete to assure one-dimensional transport. The composition and the slump of the ten examined concrete mixes are given in Table 1-10. No plasticizer was used in the preparation of the mixes having water to binder ratios 0.55. For the 0.40 ratios, plasticizer was always used in order to obtain sufficient workability; compare the measured slump values.

The chemical composition of the two examined cement clinkers is shown in Table 13 and the typical chemical composition of silica fume and fly ash, in use, is presented in Table 14.

Table 6: Mix proportions, SRPC concrete, 5 percent silica, 20 percent fly ash, water to binder ratio 0.55, slump 40 mm.

	Mass density (kg/m^3)	Weight in mix (kg)	Moisture (kg)
Cement (SRPC)	255	5.61	-
Silica	17	0.374	-
Fly ash	68	1.496	-
Aggregate 0-8 mm	882	19.50	0.09702
Aggregate 8-12 mm	917	20.17	-
Water	187	4.0170	-
Plasticizer	-	-	-

Table 7: Mix proportions, OPC concrete, water to cement ratio 0.40, slump 40 mm.

	Mass density (kg/m^3)	Weight in mix (kg)	Moisture (kg)
Cement (OPC)	440	9.68	-
Silica	-	-	-
Fly ash	-	-	-
Aggregate 0-8 mm	912	20.27	0.2025
Aggregate 8-12 mm	842	18.52	-
Water	176	3.5734	-
Plasticizer	6.60	0.1452	0.09438

Two cubes with sides 100 mm were cast for each different concrete type and sealed with plastic foil. After one day the plastic foil was removed and the samples were then stored for one week in tap water before being tested for the compressive strength. The one-week compressive strength for the concrete mixes are presented in Tables 15-17.

The slump was measured for each concrete directly after mixing using a standard cone. This was done to give a quantitative measure of the workability of the different concretes.

The three one-day membrane hardened discs from each concrete mix were either stored in tap water for one week before exposure to chlorides or stored for two weeks in air, at room temperature, followed by one week in tap water, before being submerged into the salt solution. The two 25 mm thick disks

Table 8: Mix proportions, OPC concrete, water to cement ratio 0.55, slump 40 mm.

	Mass density (kg/m^3)	Weight in mix (kg)	Moisture (kg)
Cement (OPC)	340	7.48	-
Silica	-	-	-
Fly ash	-	-	-
Aggregate 0-8 mm	971	21.49	0.1283
Aggregate 8-12 mm	861	18.94	-
Water	187	3.9858	-
Plasticizer	-	-	-

Table 9: Mix proportions, OPC concrete, 5 percent silica, water to binder ratio 0.40, slump 50 mm.

	Mass density (kg/m^3)	Weight in mix (kg)	Moisture (kg)
Cement (OPC)	418	9.20	-
Silica	22	0.484	-
Fly ash	-	-	-
Aggregate 0-8 mm	880	19.47	0.10648
Aggregate 8-12 mm	880	19.36	-
Water	176	3.6711	-
Plasticizer	6.60	0.1452	0.09438

Table 10: Mix proportions, OPC concrete, 5 percent silica, water to binder ratio 0.55, slump 40 mm.

	Mass density (kg/m^3)	Weight in mix (kg)	Moisture (kg)
Cement (OPC)	342	7.52	-
Silica	18	0.396	-
Fly ash	-	-	-
Aggregate 0-8 mm	929	20.54	0.10219
Aggregate 8-12 mm	857	18.85	-
Water	198	4.2538	-
Plasticizer	-	-	-

Table 11: Loss on ignition when heating different materials to 1050 degrees Celsius. The values are used to evaluate the degree of hydration.

Material	Loss on ignition (Percent of total)
Aggregate 0-8 mm	0.712
Aggregate 8-12 mm	0.250
Fly ash	2.153
Silica	1.304
SRPC	0.689
OPC	2.518

Table 12: Comparison between measurements using an ion-selective electrode (RCT) and titration.

Conc. Cl^-, RCT (% of concrete mass)	Conc. Cl^-, titration (% of concrete mass)	Ratio (titration/RCT)
0.640	0.721	1.13
0.530	0.592	1.12
0.390	0.424	1.09
0.300	0.323	1.08
0.215	0.218	1.01
0.145	0.156	1.08
0.096	0.096	1.00
0.054	0.063	1.17
0.037	0.043	1.16

were analyzed for hydration degree and active porosity at the same time as the 60 mm samples were exposed to a 3 wt.% sodium chloride solution.

The hydration degree, α, was measured and analyzed using the following formula

$$\alpha = \frac{W_n}{C} = \frac{W_{105}\left(1 - \left(\frac{\mu_a + \Gamma\mu_c}{1+\Gamma}\right)\right) - W_{1050}}{W_{1050} - (1-\mu_a)\left(\frac{\Gamma}{1+\Gamma}\right)W_{105}} \quad (1)$$

where W_n is the chemically bound water (kg), C is the weight of cement (kg), W_{105} is the weight after heating to 105 °C (kg), W_{1050} is the weight after heating to 1050 °C (kg), Γ is the ratio of gravel weight to cement weight, aggregate/cement (kg/kg), μ_a is the loss on ignition for gravel and

Table 13: Typical composition of the cements used.

Component	Composition SRPC (% of total)	Composition OPC (% of total)
Ca0	63.8	62.5
SiO_2	22.8	19.6
Al_2O_3	3.48	4.17
Fe_2O_3	4.74	2.17
MgO	0.80	3.45
SO_3	1.88	3.29
K_2O	0.55	1.29
Na_2O	0.06	0.26
Ignition loss	0.72	2.65

Table 14: Typical composition of silica fume and fly ash used.

Component	Composition Silica fume (Percent of total)	Composition Fly ash (Percent of total)
Ca0	0.4	1.87
SiO_2	94.2 (amorphous)	57.0
Al_2O_3	0.62	29.1
Fe_2O_3	0.95	6.56
MgO	0.65	0.79
SO_3	0.33	0.21
K_2O	0.5	1.76
Na_2O	0.2	0.28
Ignition loss	1.8	1.9

Table 15: Degree of hydration, for the water to binder ratio 0.40 concretes, at the time of exposure to chlorides. The active porosity was measured by letting the room dried samples suck water.

Concrete, w/b 0.40 (dried and rewetted before exposure to chlorides)	Degree of hydration (-)	Active porosity (-)	Comp. strength (7 d) (MPa)
SRPC	0.58	0.0691	67
SRPC, 5% silica	0.55	0.0788	66
SRPC, 5% silica 20% fly ash	0.62	0.1010	51
OPC	0.40	0.0561	62
OPC, 5% silica	0.32	0.0365	66

Table 16: Degree of hydration, for the water to binder ratio 0.55 concretes, at the time of exposure to chlorides. The active porosity was measured by letting the room dried samples suck water.

Concrete, w/b 0.55 (dried and rewetted before exposure to chlorides)	Degree of hydration (-)	Active porosity (-)	Comp. strength (7 d) (MPa)
SRPC	0.60	0.1031	38
SRPC, 5% silica	0.58	0.1070	39
SRPC, 5% silica 20% fly ash	0.64	0.1213	27
OPC	0.38	0.0736	49
OPC, 5% silica	0.34	0.0491	48

pozzolans (kg/kg) and μ_c is the loss on ignition for cement (kg/kg). The loss on ignition for the components used in the different mixes is presented in Table 11. The comparatively high value for the OPC cement examined is partially explained by the fact that 5 wt.% ground lime-stone is added to the clinker for this cement quality. The weights after heating were measured after letting the samples become equilibrated at room temperature in an exsiccator in which a very low relative humidity was obtained by using a moisture adsorbent. Formula 1 is approximative, especially when pozzolan is used in the concrete mix.

The capillary active porosity, by which is meant the porosity taking part in a short-term water adsorption test, was measured by placing one 25 mm

Table 17: Degree of hydration at the time of exposure to chlorides, water to binder ratio 0.40 concretes stored in water for 7 days before exposure.

Concrete, w/b 0.40 (stored in water before exposure to chlorides)	Degree of hydration, α (-)	Calculated porosity (-)	Comp. strength (7 d) (MPa)
SRPC	0.63	0.1177	67
SRPC, 5% silica	0.55	0.1179	66
OPC	0.40	0.1426	62
OPC, 5% silica	0.38	0.1370	66

thick plate on a free water surface after the sample had been dried in room climate for two weeks after casting. The results of the measured active porosity for the water to binder ratios 0.40 tested are shown in Table 15. The corresponding results for the 0.55 ratios are presented in Table 16. The samples never dried before exposure to chlorides were not analyzed by this method. The total weight gain due to capillary sucked water, when equilibrium was reached, was used as a quantitative measure of the active porosity. The initial water content in sample before capillary suction test is not included in the evaluation of the active porosity.

The total porosity of samples never dried before exposure was estimated by considering the cement content in the mix, the water to binder ratio and the measured hydration degree at the time of exposure, using the formula: $P_{tot} = C/1000(w/b - 0.19\alpha)$, where C is the mass density concentration of cement in mix, w/b is the water to binder ratio and α is the degree of hydration. The values obtained for the degree of hydration and calculated total porosities are presented in Table 17.

After the two different curing conditions were completed, the 60 mm thick samples, having the PVC cylinder mold covering the envelope sides, were submerged in a 3 wt.% sodium chloride solution. The exposure solution was replaced twice during the test period of 119 days.

After 119 days of exposure, the samples were taken out of the chloride bath and wiped off with a rag. Only samples having sawn surfaces were examined, that is, no samples with a cast surface was tested. Indeed, a significant difference of chloride penetration profiles in samples having sawn exposed surfaces or cast surfaces has been observed, [17]. This is presumably caused by an enrichment of cement near the exposed cast surface. After removal

Table 18: Calibration curves for the ion-selective electrode for the samples dried for 14 days and stored in pure water for 7 days before exposure to chlorid.

Concrete	Calibration curve (mass percent Cl^- by concrete mass)
SRPC, w/c 0.40	$C_{Cl} = 0.3982 \exp(-0.04223U)$
SRPC, 5% silica, w/b 0.40	$C_{Cl} = 0.4283 \exp(-0.04238U)$
SRPC, 5% silica 20% fly ash, w/b 0.40	$C_{Cl} = 0.4476 \exp(-0.04303U)$
OPC, w/c 0.40	$C_{Cl} = 0.4336 \exp(-0.04289U)$
OPC, 5% silica, w/b 0.40	$C_{Cl} = 0.4476 \exp(-0.04303U)$
SRPC, w/c 0.55	$C_{Cl} = 0.3982 \exp(-0.04223U)$
SRPC, 5% silica, w/b 0.55	$C_{Cl} = 0.4283 \exp(-0.04238U)$
SRPC, 5% silica 20% fly ash, w/b 0.55	$C_{Cl} = 0.4336 \exp(-0.04289U)$
OPC, w/c 0.55	$C_{Cl} = 0.4336 \exp(-0.04289U)$
OPC, 5% silica, w/b 0.55	$C_{Cl} = 0.4476 \exp(-0.04303U)$

Table 19: Calibration curves for the ion-selective electrode for the samples stored in pure water for 7 days before exposure to chlorid.

Concrete	Calibration curve (mass percent Cl^- by concrete mass)
SRPC, w/c 0.40	$C_{Cl} = 0.4196 \exp(-0.04232U)$
SRPC, 5% silica, w/b 0.40	$C_{Cl} = 0.4298 \exp(-0.04157U)$
OPC, w/c 0.40	$C_{Cl} = 0.3982 \exp(-0.04223U)$
OPC, 5% silica, w/b 0.40	$C_{Cl} = 0.4270 \exp(-0.04154U)$

Table 20: Total chloride profile, SRPC concrete, water to cement ratio 0.40. Concrete dried for 14 days and rewetted for 7 days before being exposed to a 3 weight percent sodium chloride solution for 119 days.

Depth (mm)	U (mV)	Total Cl^- (wt % of concrete)
0.0-0.7	2.1	0.364
0.7-1.4	-0.7	0.410
1.4-2.5	1.7	0.371
2.5-4.2	5.4	0.317
6.6-8.1	15.4	0.208
10.8-12.0	31.4	0.106
15.7-16.6	63.9	0.027
21.5-23.3	116.8	0.003
27.6-29.4	118.7	0.003

from the storage solution, the sample was fixed into a grinding device where approximately 1.2 mm thick layers were collected. Layers were collected to a total depth of approximately 30 mm from the exposed surface. The concrete powder collected from each layer was stored in marked sealed plastic bags. The depth from surface was measured for each removed layer using a slide-calliper measuring the depth at various locations; the mean value of these measurements were used.

The concrete powder was analyzed for total chloride content by using the rapid chloride test method, RCT. 1.5 ± 0.005 gram of the ground concrete dust was placed in a small bottle containing 10 ml of an dissolving liquid. The bottles were shaken for approximately 10 minutes. The chloride content was then measured by placing an ion-selective electrode in the solution and a measure in terms of volts was registered. The electrode was calibrated before and after each test series, using reference solutions at four different known concentrations. The difference of the values in the calibration before and after testes was allowed to be 3-5 mV for low concentrations and 1-2 mV for the highest concentrations. The obtained calibration curves for the different tests performed are presented in Tables 18 and 19.

The measured total chloride profiles, after 119 days of exposure, for concretes based on SRPC are presented in Tables 20-25. These samples were dried for 14 days and rewetted in tap water for 7 days before exposure. The

Table 21: Total chloride profile, SRPC concrete, water to cement ratio 0.55. Concrete dried for 14 days and rewetted for 7 days before being exposed to a 3 weight percent sodium chloride solution for 119 days.

Depth (mm)	U (mV)	Total Cl^- (wt % of concrete)
0.0-1.1	7.3	0.293
1.1-2.3	5.5	0.316
2.3-3.5	5.4	0.317
3.5-5.4	6.1	0.308
5.6-7.2	13.2	0.228
7.2-9.5	18.2	0.185
9.8-11.8	20.6	0.167
17.2-19.4	40.5	0.072
24.7-27.1	68.1	0.022
27.1-29.5	84.4	0.011

Table 22: Total chloride profile, SRPC concrete with 5 percent silica fume, water to binder ratio 0.40. Concrete dried for 14 days and rewetted for 7 days before being exposed to a 3 weight percent sodium chloride solution for 119 days.

Depth (mm)	U (mV)	Total Cl^- (wt % of concrete)
0.0-0.9	19.0	0.191
0.9-1.8	14.1	0.236
1.8-2.6	13.9	0.238
2.6-4.0	15.2	0.225
4.0-6.0	19.8	0.185
6.0-7.5	27.6	0.133
10.1-11.0	60.7	0.033
15.1-16.5	116.6	0.003
22.1-24.3	120.9	0.003
28.9-30.2	121.1	0.003

Table 23: Total chloride profile, SRPC concrete with 5 percent silica fume, water to binder ratio 0.55. Concrete dried for 14 days and rewetted for 7 days before being exposed to a 3 weight percent sodium chloride solution for 119 days.

Depth (mm)	U (mV)	Total Cl^- (wt % of concrete)
0.0-1.0	22.8	0.163
1.0-2.0	19.4	0.188
2.0-2.9	20.6	0.179
2.9-4.1	20.9	0.177
4.1-5.1	22.4	0.166
6.6-8.5	32.1	0.110
10.7-12.3	46.9	0.059
16.1-17.5	78.4	0.015
21.9-23.7	118.6	0.003
27.0-29.6	120.9	0.003

Table 24: Total chloride profile, SRPC concrete with 5 percent silica fume and 20 percent fly ash, water to binder ratio 0.40. Concrete dried for 14 days and rewetted for 7 days before being exposed to a 3 weight percent sodium chloride solution for 119 days.

Depth (mm)	U (mV)	Total Cl^- (wt % of concrete)
0.0-1.2	19.8	0.191
1.2-1.9	18.7	0.200
1.9-2.9	20.3	0.187
2.9-3.8	22.4	0.171
3.8-5.8	26.0	0.146
5.8-7.3	30.7	0.119
7.3-8.0	35.4	0.098
9.4-11.1	57.2	0.038
12.7-14.4	93.6	0.008
16.6-18.6	115.4	0.003
22.0-23.5	122.7	0.002
26.8-29.0	117.6	0.003

Table 25: Total chloride profile, SRPC concrete with 5 percent silica fume and 20 percent fly ash, water to binder ratio 0.55. Concrete dried for 14 days and rewetted for 7 days before being exposed to a 3 weight percent sodium chloride solution for 119 days.

Depth (mm)	U (mV)	Total Cl^- (wt % of concrete)
0.0-1.5	25.6	0.145
1.5-2.7	19.8	0.185
2.7-4.6	20.0	0.184
4.6-6.2	24.4	0.152
6.2-7.7	26.1	0.142
7.7-9.7	31.7	0.111
9.7-11.7	43.3	0.068
13.0-15.0	62.8	0.029
17.2-19.1	92.8	0.008
22.4-24.5	122.2	0.002
28.8-30.7	124.0	0.002

calibration constants in use are shown in Table 18. Results for the OPC concretes exposed to the same pre-conditioning as above are shown in Tables 26-29 and the corresponding measured calibration curves are presented in Table 18.

The obtained total chloride profiles for concretes based on SRPC and OPC, being stored for 7 days in tap water before exposure, are presented in Tables 30-31 and Tables 32-33, respectively. The calibration values for these measurements are shown in Table 19.

A series of measurements were carried out with both the RCT method described above and with a traditional titration using a CIBA-CORNING 926 Chloride Analyzer. In this method silver ions are supplied to the test container from a silver anode using a constant current. A 'dead stop' system is used, i.e. when all the chloride ions in the solution have been consumed by the silver ions the indicator electrode stops the current. The total registered time of supplying the constant current through the solution serves as a measure of the amount of chloride ions in the sample.

A comparison between results of measurements using the RCT-method and the titration is shown in Table 12. In general, the RCT-method gave

Table 26: Total chloride profile, OPC concrete, water to binder ratio 0.40. Concrete dried for 14 days and rewetted for 7 days before being exposed to a 3 weight percent sodium chloride solution for 119 days.

Depth (mm)	U (mV)	Total Cl^- (wt % of concrete)
0.0-1.4	16.2	0.216
1.4-2.9	13.7	0.241
2.9-4.0	14.1	0.237
4.0-5.0	16.7	0.212
5.0-6.7	20.3	0.182
6.7-8.3	23.4	0.159
8.3-10.1	29.8	0.121
10.1-11.1	40.7	0.076
14.3-16.4	83.8	0.012
21.9-23.8	121.9	0.002
28.2-29.9	122.8	0.002

Table 27: Total chloride profile, OPC concrete, water to binder ratio 0.55. Concrete dried for 14 days and rewetted for 7 days before being exposed to a 3 weight percent sodium chloride solution for 119 days.

Depth (mm)	U (mV)	Total Cl^- (wt % of concrete)
0.0-1.7	23.6	0.158
1.7-3.1	21.2	0.175
3.1-4.5	20.3	0.182
4.5-6.2	24.5	0.152
6.2-7.7	26.5	0.139
7.7-9.6	28.1	0.130
9.6-11.3	32.0	0.110
13.6-15.3	41.2	0.074
18.3-20.6	65.2	0.026
25.0-29.1	117.7	0.003

Table 28: Total chloride profile, OPC concrete with 5 percent silica fume, water to binder ratio 0.40. Concrete dried for 14 days and rewetted for 7 days before being exposed to a 3 weight percent sodium chloride solution for 119 days.

Depth (mm)	U (mV)	Total Cl^- (wt % of concrete)
0.0-1.6	16.9	0.216
1.6-2.6	16.3	0.222
2.6-3.6	21.0	0.181
3.6-4.8	27.2	0.139
4.8-5.9	35.9	0.096
5.9-7.8	47.2	0.059
7.8-9.0	60.6	0.033
9.0-10.7	75.6	0.017
11.9-13.4	105.5	0.005
15.3-17.2	116.1	0.003
21.7-23.0	117.2	0.003
26.8-28.8	118.7	0.003

Table 29: Total chloride profile, OPC concrete with 5 percent silica fume, water to binder ratio 0.55. Concrete dried for 14 days and rewetted for 7 days before being exposed to a 3 weight percent sodium chloride solution for 119 days.

Depth (mm)	U (mV)	Total Cl^- (wt % of concrete)
0.0-1.3	24.8	0.154
1.3-2.2	22.6	0.169
2.2-3.7	23.0	0.166
3.7-5.3	23.8	0.161
5.3-6.8	30.8	0.119
6.8-8.4	38.2	0.087
8.4-9.8	47.7	0.057
9.8-11.7	61.2	0.032
15.0-16.7	108.9	0.004
20.1-21.6	120.3	0.003
26.7-30.1	120.3	0.003

significantly lower values of the chloride content than the titration. The differences between the methods seem to be more dominant for the high and low concentrations compared to the medium concentrations tested. The reason between the discrepancy was not analyzed.

3 Description of the model

Most existing models of chloride penetration into cement-based materials use the effective diffusivity for chlorides in material together with Fick's second law. The effective diffusion coefficient includes binding of chlorides for cases when the binding is instantaneous and the chloride binding isotherm is linear. Comparisons between models and experiment forces the effective diffusion coefficient to be a function of chloride content, e.g. see [18], [19] and [20], the moisture content, e.g. see [2] and the exposure time, e.g. see [21]. Instead of using the classical effective diffusivity concept a method will be tested where the known bulk diffusion coefficients of different types of ions are scaled with a tortuosity factor which take into account the porosity and the shape of the water filled pore system and the binding will be treated with separate

Table 30: Total chloride profile, SRPC concrete, water to cement ratio 0.40. Cured in tap water for 7 days before exposure to a 3 weight percent sodium chloride solution for 119 days.

Depth (mm)	U (mV)	Total Cl^- (wt % of concrete)
0.0-1.0	-2.5	0.466
1.0-2.4	-1.8	0.453
2.4-3.3	0.0	0.420
5.9-7.6	11.6	0.257
11.8-13.0	25.8	0.141
15.7-17.8	48.4	0.054
22.4-24.6	99.9	0.006
27.5-29.3	116.6	0.003

Table 31: Total chloride profile, SRPC concrete with 5 percent silica fume, water to binder ratio 0.40. Cured in tap water for 7 days before exposure to a 3 weight percent sodium chloride solution for 119 days.

Depth (mm)	U (mV)	Total Cl^- (wt % of concrete)
0.0-1.2	-2.8	0.483
1.2-2.1	-1.1	0.450
2.1-3.6	1.2	0.409
3.8-5.5	12.0	0.261
5.9-6.5	15.6	0.225
6.5-8.1	20.0	0.187
12.5-14.1	53.2	0.047
18.3-19.8	107.4	0.005
23.9-26.6	118.2	0.003
26.6-30.0	119.9	0.003

Table 32: Total chloride profile, OPC concrete, water to cement ratio 0.40. Cured in tap water for 7 days before exposure to a 3 weight percent sodium chloride solution for 119 days.

Depth (mm)	U (mV)	Total Cl^- (wt % of concrete)
0.0-0.7	-5.4	0.500
0.7-1.8	-4.9	0.490
1.8-3.2	0.3	0.393
3.2-4.3	2.8	0.354
6.1-7.4	10.1	0.260
10.3-11.2	25.6	0.135
13.5-14.8	51.3	0.046
19.8-21.6	94.9	0.007
26.6-29.2	113.9	0.003

Table 33: Total chloride profile, OPC concrete with 5 percent silica fume, water to binder ratio 0.40. Cured in tap water for 7 days before exposure to a 3 weight percent sodium chloride solution for 119 days.

Depth (mm)	U (mV)	Total Cl^- (wt % of concrete)
0.0-0.8	5.5	0.340
0.8-1.8	-0.4	0.434
1.8-2.9	4.4	0.356
2.9-4.2	10.0	0.282
4.2-5.8	15.1	0.228
8.7-10.0	59.6	0.036
15.0-17.1	119.6	0.003
22.7-25.0	123.2	0.003
25.0-29.7	123.0	0.003

Table 34: Pore extraction data for a 5-month-old concrete with water to binder ratio 0.40. The concrete was stored in water during the whole time.

Specimen w/b 0.4	Silica (%)	Fly ash (%)	ICP K^+ (mmol/l)	ICP Na^+ (mmol/l)	Titration OH^- (mmol/l)	(Error) (mmol/l)
SRPC	-	-	445	42	482	5
SRPC	5	-	225	34	286	3
SRPC	5	10	264	50	281	15
OPC	-	-	752	122	860	14

constitutive relations.

The model to be described in this section includes a set of material constants. These constants will later be chosen in a way giving the best fit to the measured data presented in section 2. The model includes dielectrical effects among ions dissolved in pore solution of the concrete. Therefore it is important to include as many of the different ions appearing in the pore solution as possible. Here five different ions will be considered. The five different types of ions of interest are Cl^- (1), Na^+ (2), OH^- (3), Ca^{2+} (4) and K^+ (5), where the ions have been given numbers ranging from 1 to 5 for ease of notation. Furthermore, two solid constituents are included, i.e. $CaCl_2$ (6) and $Ca(OH)_2$ (7). These constituents will be denoted by the numbers 6 and 7.

Loosely speaking, the model consists of two parts. The first is concerned with the description of the mass flow of ions dissolved in pore solution. These types of flow will be assumed to depend on two different 'forces', a mole density concentration gradient driven flow and a flow caused by a gradient of the electro-static potential. An electrostatic potential field will be assumed developed in the domain due to positively and negatively charged ions being transported in the pore solution. No external electrical forces will be included. The second part of the model consists of a description of the mass exchange between solid constituents and dissolved ions in pore solution. These chemical reactions include a description of equilibrium conditions, i.e. in which conditions the chemical reaction rate is zero, and a description of the kinetics of the reactions before reaching equilibrium. Chemical reactions among the different types of ions appearing in pore solution will not be included in the model.

Table 35: Constants for ions dissolved in bulk water at room temperature.

Substance	Diffusion coeff. D (m^2/s)	Ionic mobility A ($m^2/s/V$)	Dielectricity coeff. $\varepsilon\varepsilon_0$ (C/V)
Cl^-	$2.03 \cdot 10^{-9}$	$7.91 \cdot 10^{-8}$	-
OH^-	$5.30 \cdot 10^{-9}$	$20.64 \cdot 10^{-8}$	-
Na^+	$1.33 \cdot 10^{-9}$	$5.19 \cdot 10^{-8}$	-
K^+	$1.96 \cdot 10^{-9}$	$7.62 \cdot 10^{-8}$	-
Ca^{2+}	$0.79 \cdot 10^{-9}$	$6.17 \cdot 10^{-8}$	-
H_2O	-	-	$695.4 \cdot 10^{-12}$

The chloride ions in pore solution are assumed to be able to get bound into the calcium hydroxide sheets, being intergrown with the cement gel, by ion exchange according to the following formula:

$$X \cdot (Ca(OH)_2)(s) + 2Cl^-(aq) \longrightarrow 2OH^-(aq) + X \cdot (CaCl_2)(s) \qquad (2)$$

where X denotes other solid hydration products than crystalline calcium hydroxide. It should be noted that the ion exchange reaction (2) is only one possible cause of chloride binding. Other mechanisms such as physical binding and creation of so-called double layers have been proposed as the main reason for binding of chlorides in the micro-structure of concrete. In this study, however, only the effect of assuming reaction (2) to be valid will be examined.

The dissolution reaction (2) is assumed active when the actual value of the concentration of chloride ions in pore solution is lower than a certain equilibrium value which will be assumed to depend on the actual concentration of solid calcium hydroxide.

When reaction (2) not is active, depending on the relation of the concentration of dissolved chloride ions and chloride bound in the solid structure, dissolution of chlorides is assumed according to reaction (3). That is, chloride ions from already formed solid calcium chloride are assumed to be able to be dissolved forming dissolved calcium and chloride ions, i.e.

$$X \cdot (CaCl_2)(s) \longrightarrow Ca^{2+}(aq) + 2Cl^-(aq) + X(s) \qquad (3)$$

The third and last considered chemical reaction is dissolution of calcium hydroxide from the hydration products. The reaction is assumed to be re-

versible, as

$$\mathrm{X}\cdot\left(\mathrm{Ca}\left(\mathrm{OH}\right)_2\right)(\mathrm{s}) \rightleftarrows \mathrm{Ca}^{2+}(\mathrm{aq})+2\mathrm{OH}^{-}(\mathrm{aq})+\mathrm{X}(\mathrm{s}) \tag{4}$$

It will be assumed that an equilibrium condition exists in which no reactions involving chloride ions takes place. This relation is assumed to be dependent on the concentration of dissolved chloride ions in pore solution n_1, bound chlorides n_6 and the concentration of dissolved hydroxide ions in pore solution n_3. The relation $n_1^{eq} = (K + Zn_3)\, n_6$ will be used, which constitutes a binding isotherm for chlorides expressed with the material constants K and Z. The property n_1^{eq} stands for the special condition in terms of the concentration of chloride, in pore solution, when no mass exchange of dissolved and bound chlorides occurs. The inclusion of the term Zn_3 makes it possible to include the effect of the pH-value in pore solution on the binding characteristics of chlorides. When having a concentration of dissolved chlorides ions lower than its equilibrium concentration, chlorides will continue to be bound into the solid structure until the equilibrium is obtained, i.e. when $n_1^{eq} \leq n_1$ the reaction described in (2) will be assumed to take place. On the other hand, if the equilibrium condition n_1^{eq} is exceeded, chloride ions will be dissolved from the solid according to the assumed reaction (3).

Under the condition that the equilibrium value for the concentration of dissolved chloride ions n_1^{eq} is lower than the actual value of the chloride concentration n_1, i.e. $n_1^{eq} \leq n_1$, the equation describing the dissolved chloride ions in pore solution is given as

$$\begin{aligned}\frac{\partial n_1}{\partial t} &= \mathrm{div}\left(\tilde{D}_1 \mathrm{grad} n_1 + \tilde{A}_1 v_1 n_1 \mathrm{grad}\varphi\right) \\ &\quad + R\left(\left(K + Zn_3\right) n_6 - n_1\right)\end{aligned} \tag{5}$$

where $\tilde{D}_1$ is the scaled value of the diffusion coefficient for chlorides, i.e. $\tilde{D}_1 = tD_1$, where D_1 is the diffusion coefficient for chloride ions in bulk water, e.g. see [22], [23] and Table 35, and t is the tortuosity factor. The material constant $\tilde{A}_1$ is the scaled ionic mobility coefficient for chloride ions dissolved in pore solution and v_1 denotes the valence number, which for chloride ions is equal to -1. The state variable denoted φ, present in equation (5), is the electric potential in the mixture, which will be solved using equation (12). The assumptions leading to the governed equation for φ will be explained at the end of this section. The material constant R denotes the rate constant when reaction (2) is active. This means, according to the last

term in equation (5), that the rate of production of bound chlorides is proportional to the 'distance' from the current equilibrium condition defined by $n_1^{eq} = (K + Zn_3)\, n_6$, where n_3 and n_6 is the concentration of hydroxide ions in pore solution and concentration of solid calcium chloride in the hydrated cement, respectively.

In cases when $n_1^{eq} > n_1$ it is assumed that dissolution of chlorides occurs according to reaction (3). The dissolution rate is assumed to be proportional to the 'distance' from the current equilibrium condition, in the same manner as for binding of chlorides. The dissolution rate of chlorides is, however, assumed to be significantly different from the process of binding of chlorides. This is tackled by replacing the rate constant R, in equation (5), by S, whenever $n_1^{eq} > n_1$. The material constant S represents the rate constant for reaction (3). Naturally, it is possible to set the material constants R and S to values which reproduce a case where equilibrium is established instantaneously, or very close to being instantaneous. That is, the most common way of treating binding of chlorides can be obtained as a special case, by neglecting the reaction kinetics, by setting R and S to high values.

The equation for determination of the mole density concentration for dissolved sodium ions in pore solution n_2, is given as

$$\frac{\partial n_2}{\partial t} = \mathrm{div}\left(\tilde{D}_2 \mathrm{grad} n_2 + \tilde{A}_2 v_2 n_2 \mathrm{grad}\varphi\right) \tag{6}$$

where $\tilde{D}_2$ and $\tilde{A}_2$, again, stand for the scaled diffusion coefficient and ionic mobility for the sodium ions, respectively. The direction of the flow caused by the second terms on the right hand side of equation (6), i.e. caused by the gradient of the electric potential, is noted to be of opposite sign than compared to the same term appearing in equation (5) describing the chlorides. This is taken into account explicitly, by applying the correct positive or negative number of the valence, in this case for v_1 (negative) and v_2 (positive).

It is noted that the sodium ions dissolved in pore solution are not involved in any of the assumed chemical reactions, i.e. sodium ions are not included in reactions (2), (3) and (4). Therefore the action of sodium ions is determined solely by diffusion caused by its concentration gradient and the gradient of the electrical potential φ. Further, it can be concluded that the condition of the concentration of sodium ions at different material points and at different time levels, which is to be calculated with equation (6), will affect the distribution of chloride ions since the electric potential φ, determined by the composition of the mixture, couples all equations for the different types of ions.

The hydroxide ions, dissolved in the pore solution, whose concentration is denoted n_3, will be given, not only by their gradient-dependent flow characteristics, but also by the chemical reactions (2) and (4). That is, a hydroxide ion is supplied to the pore solution for every chloride ion being bound as assumed in reaction (2). Hydroxide ions are, further, either supplied or consumed from the pore solution according to reaction (4). The equilibrium condition of hydroxide ions in pore solution n_3^{eq} is assumed as $n_3^{eq} = Wn_7$, where W is a material constant and n_7 is the mole density concentration of solid calcium hydroxide, i.e. when $n_3^{eq} = n_3$ the reaction (4) is not active. When the actual concentration of hydroxide n_3 is smaller than its corresponding equilibrium value n_3^{eq}, which is a function of the concentration of solid calcium hydroxide, hydroxide ions will be supplied to the pore solution. It is also assumed that hydroxide can be bound into the solid structure when $n_3^{eq} < n_3$, but such situations are rare since, normally, the only source of hydroxide ions is the internal solid hydration products.

Under the condition $n_1^{eq} \leq n_1$ the hydroxide ion concentration in pore solution is described as

$$\begin{aligned} \frac{\partial n_3}{\partial t} &= \operatorname{div}\left(\tilde{D}_3 \operatorname{grad} n_3 + \tilde{A}_3 v_3 n_3 \operatorname{grad}\varphi\right) \\ &\quad -Q\left(Wn_7 - n_3\right) - R\left(\left(K + Zn_3\right) n_6 - n_1\right) \end{aligned} \tag{7}$$

where $n_3^{eq} = Wn_7$ and $n_1^{eq} = \left(K + Zn_3\right) n_6$. The rate constant Q is associated with the reaction (4), i.e. the rate of dissolution of calcium and hydroxide from solid is assumed to be proportional to the difference between the actual concentration of hydroxide n_3 and the corresponding equilibrium value n_3^{eq}. Under conditions when $n_1^{eq} > n_1$ the material constant R, in equation (7), is set to zero, since no supply of hydroxide ions to pore solution occurs when reaction (3) is active.

On condition that the equilibrium concentration of chloride ions in pore solution is higher than the actual value, i.e. if $n_1^{eq} > n_1$, the equation for the determination of the concentration field of calcium ions in pore solution, is given as

$$\begin{aligned} \frac{\partial n_4}{\partial t} &= \operatorname{div}\left(\tilde{D}_4 \operatorname{grad} n_4 + \tilde{A}_4 v_4 n_4 \operatorname{grad}\varphi\right) \\ &\quad -\tfrac{1}{2}Q\left(Wn_7 - n_3\right) + \tfrac{1}{2}S\left(\left(K + Zn_3\right) n_6 - n_1\right) \end{aligned} \tag{8}$$

When $n_1^{eq} \leq n_1$ the rate constant S is set to zero because the reaction described in (3) is not active in this case. Depending on the relation between

the actual value of the hydroxide ion concentration in pore solution n_3 and its equilibrium value n_3^{eq}, calcium ions are either supplied or removed from pore solution, according to the chemical reaction (4) and the term $\frac{1}{2}Q\left(Wn_7 - n_3\right)$ in equation (8). In situations when the equilibrium concentration and the actual concentration of chloride ions in pore solution is related as $n_1^{eq} > n_1$, the reaction (3) is assumed to be active. Hence, one calcium ion will be supplied to the pore solution for every two chloride ions dissolved from the solid calcium chloride.

The governed equation for the dissolved potassium ion concentration in pore solution n_5 is given as

$$\frac{\partial n_5}{\partial t} = \mathrm{div}\left(\tilde{D}_5 \mathrm{grad} n_5 + \tilde{A}_5 v_5 n_5 \mathrm{grad}\varphi\right) \tag{9}$$

The potassium ions appearing in pore solution are not assumed to be involved in any chemical reactions, i.e. compare with reactions (2), (3) and (4).

It will be explicitly assumed that the diffusion velocity for the solid $CaCl_2$ component is zero. That is, the differential equation describing the rate of change of the mole density of $CaCl_2$ is only due to chemical reactions. If the condition $n_1^{eq} \leq n_1$ holds, the governed equation for the solid calcium chloride concentration will be given as

$$\frac{\partial n_6}{\partial t} = -\frac{1}{2}R\left(\left(K + Zn_3\right)n_6 - n_1\right) \tag{10}$$

which mean that production of solid calcium chloride takes place, according to reaction (2), whenever the equilibrium concentration of chloride ions in pore solution is smaller than its corresponding actual value. When having $n_1^{eq} > n_1$, the rate constant R for binding of chlorides is replaced by the rate constant S associated with dissolution of chlorides from already formed solid calcium chloride. This means, further, that the reaction involving solid calcium chloride (2) is replaced by (3), which describes dissolution of calcium and chloride ions from solid.

The solid calcium hydroxide constituent is, also, assumed to have zero diffusion velocity. In conditions when $n_1^{eq} \leq n_1$ the description of the solid calcium hydroxide concentration n_7 is obtained as

$$\frac{\partial n_7}{\partial t} = \frac{1}{2}Q\left(Wn_7 - n_3\right) + \frac{1}{2}R\left(\left(K + Zn_3\right)n_6 - n_1\right) \tag{11}$$

That is, reaction (4), contributing either to a supply or a decrease of solid calcium hydroxide, and reaction (2), contributing to a decrease of solid calcium-hydroxide due to ion exchange, are assumed to be active. In the other possible

condition, i.e. when $n_1^{eq} > n_1$, the rate constant R is set to zero, since no consumption or production of solid calcium hydroxide occurs when reaction (3) is active.

The last information needed is the equation describing the electrostatic potential φ, The governing equation for the static electropotential can be obtained by using constitutive relations together with the static continuity equation for the charge, which is one of Maxwell's equations. It is assumed that the so-called electric displacement vector is related to the gradient of the electrostatic potential φ through the material constant $\tilde{\varepsilon}\varepsilon_0$, referred to as the permittivity or the dielectric coefficient. The property ε_0 is the permittivity of vacuum, $\varepsilon_0 = 8.854 \cdot 10^{-12}$, and $\tilde{\varepsilon}$ is the relative coefficient that varies among different mediums. For water at 25°C, $\tilde{\varepsilon}\varepsilon_0 = 695.4 \cdot 10^{-12}$. The so-called charge density q is assumed to be given by: $q = F \sum_{a=1}^{5} n_a(x,t)\, v_a$, where F is the charge of one mole of an ion having the valence number v_a. That is, the charge density, at every material point and at every time level, is assumed to be given by the composition of the mixture in terms of concentrations of positive and negatively charged ions in pore solution. The resulting equation used for determining the electrostatic potential φ is obtained by introducing the assumptions described above into the continuity equation for the charge, and the result is

$$-\mathrm{div}\left(\tilde{\varepsilon}\varepsilon_0 \mathrm{grad}\varphi\right) = F \sum_{a=1}^{5} n_a(x,t)\, v_a, \tag{12}$$

It is noted that equation (12) needs the information on the concentrations of the five different dissolved ions in pore solution. These different concentrations are calculated from equations (5), (6), (7), (8) and (9). Further, it should be observed that the same five equations cannot be solved without having knowledge about the electrostatic potential φ at all material points and at every time level. This means that the equations for the charged constituents dissolved in pore solution and the equation (12) for the electrostatic potential φ are coupled in both directions.

Excluding the physical constant F, the model includes in total 17 material constants. The description of the velocity of the dissolved ions involves 5 diffusion constants and 5 ionic mobility constants; the description leading to a determination of the electrostatic potential involves one constant, i.e. the property $\tilde{\varepsilon}\varepsilon_0$; the description of the chemical equilibrium conditions involves 3 constants, i.e. K, Z and W; and the description of the kinetics of the

considered chemical reactions involves 3 rate constants, i.e. R, S and Q.

Boundary conditions and initial conditions need to be specified in the above equations. The initial condition are the description of the initial concentrations of dissolved OH^-, Ca^{2+}, Na^+ and K^+, and solid $Ca(OH)_2$ (assuming the concentration of dissolved Cl^- and solid $CaCl_2$ initially to be zero). The boundary conditions are the description of the concentration of different types of ions in the outer storage solution (or a description of the mass density flow conditions at the boundary); these concentrations can be allowed to change with time. The outer storage solution, described by the boundary condition, is always assumed to consist of a neutral combination of positive and negatively charged ions. By assuming this one can justify having a boundary condition, in terms of the electrostatic potential φ, set to zero at the surface exposed to the ion solution, compare equation (12).

A phenomenon ignored in the development of the governing equations, in this section, is the solubility properties of the mixture of different types of ions in bulk water. The case is that neutrally charged packages of ions will be deposited on the pore walls if the solubility of the mixture of ions in pore solution is exceeded. It might be the case that such effects, influencing the description of the system, are as important as the chemical reactions (or physical binding of ions onto the solid products) considered in the proposed model. Yet another phenomenon, which may be studied and included in a model concerning diffusion of different types of ions in concrete, is the development of so-called double layers on pore wall surfaces.

4 Test results

The Finite Element Method, FEM, is used to solve the transient coupled equations, described in section 3. Simple linear one-dimensional elements are used. The semi-discretization is performed with a single time step method using an implicit weighting in the time domain. The non-linearities, mainly caused by the inclusion of the dielectrical effects, are treated by a simple explicit method. The coupling between the different constituent equations is solved by arranging the individual 'stiffness' matrixes as block matrixes in which the off-diagonal block matrixes represent the coupling terms. This means that nodal values for all different constituents, at each time level, can be calculated in one step only. The effect of the non-linearities on the solution has been controlled by simply testing smaller and smaller time steps

until the solutions converge. The Finite Element Method as a tool for solving transient problems can be studied in, for example, [24], [25] and [26].

The initial conditions in terms of mole concentrations of ions in pore solution, i.e. the mole density concentration of K^+, Na^+, OH^- and Ca^+, are based on the measured pore extraction data given in Table 34. These experiments were performed by EUROC RESEARCH. The outer concentrations of sodium and chloride ions are set to 510 mol/m^3, during all time steps in the simulation, which is the conditions used in the tests assuming that the consumption of sodium and chloride ions in storage solution affects the global concentration very little.

The boundary conditions in terms of mole density concentrations for the ion constituents K^+, OH^- and Ca^+ are set to zero, which assumes that other ions than sodium and chloride ions being leached to the surrounding storage solution affect the overall diffusion behavior to a small extent. This assumption is fairly reasonable for the test performed since the volume of the sodium chloride storage solution is very large compared to the sample size.

The electrostatic potential field is solved by letting the surface exposed to the sodium chloride solution have a known potential prescribed as zero. This implies that the net charge imbalance among the ions dissolved being transported through the boundary surface is very close to zero at every time level.

Even though the determination of the simulated total chloride profiles at certain exposure times requires the determination of bound and free concentrations of chlorides, together with determination of all other included constituent concentration fields, which becomes necessary due to the chemical reactions and dielectrical effects assumed, only the total chloride profiles, after 119 days of exposure to a 3 wt.% sodium chlorides solution, will be presented.

The one-dimensional domain with symmetrically applied boundary conditions is divided into two symmetrical regions in which a zero mass flow has been prescribed at the middle of the domain. This type of boundary conditions are used for all considered constituents.

The diffusion coefficients and ion mobility coefficients presented in Table 35 are used together with one tortuosity factor modeling the damping of the diffusion velocities due to the porosity and due to the shape of the pore system. It is, therefore, assumed that different ions being dissolved in the pore solution are affected by the porosity and the shape of the pore system in the same manner. This approach becomes possible since the chemical reactions

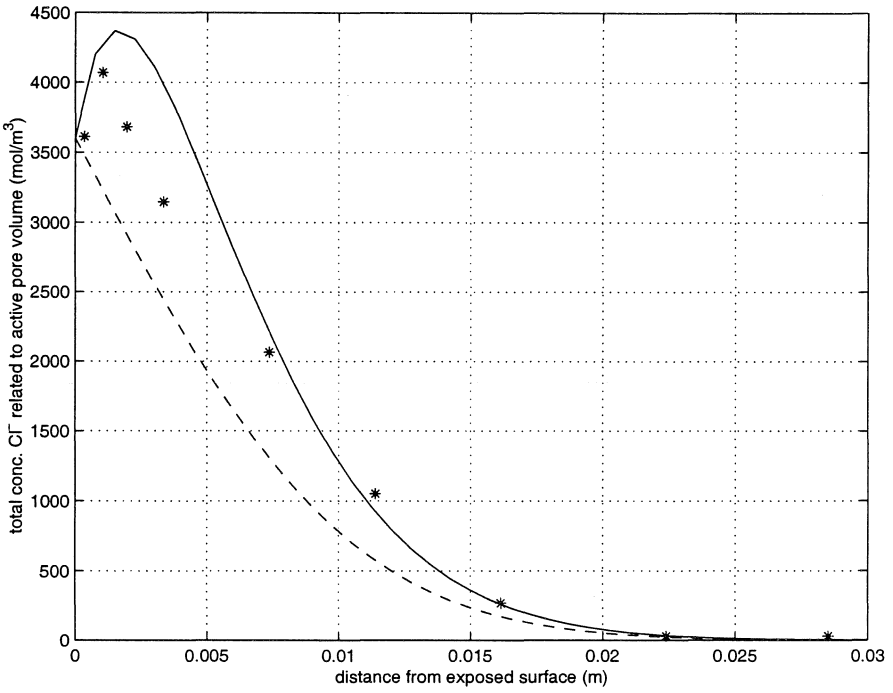

Figure 1: *SRPC concrete, water to cement ratio 0.40, exposed for 119 days to 3 wt.% sodium chloride solution. The concrete sample was dried for 14 days and rewetted for 7 days in tap water before being exposed to chlorides. The solid line represents simulated results for total chloride concentration as related to active water-filled volume. The dashed line is the simulated result when excluding dielectric effects. The stars represent measured values as related to active water-filled volume.*

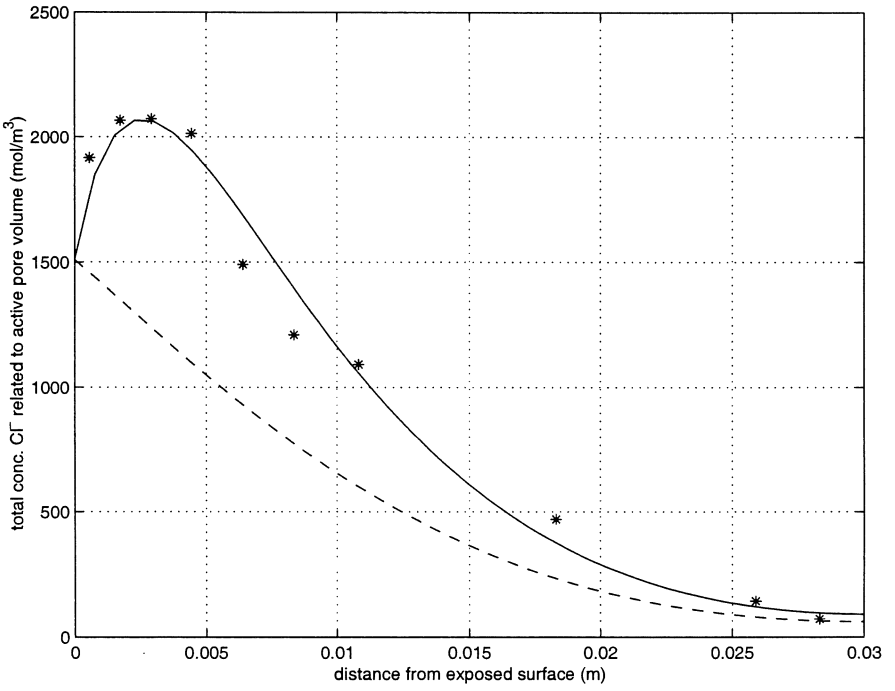

Figure 2: *SRPC concrete, water to cement ratio 0.55, exposed for 119 days to 3 wt.% sodium chloride solution. The concrete sample was dried for 14 days and rewetted for 7 days in tap water before being exposed to chlorides. The solid line represents simulated results for total chloride concentration as related to active water-filled volume. The dashed line is the simulated result when excluding dielectric effects. The stars represent measured values as related to active water-filled volume.*

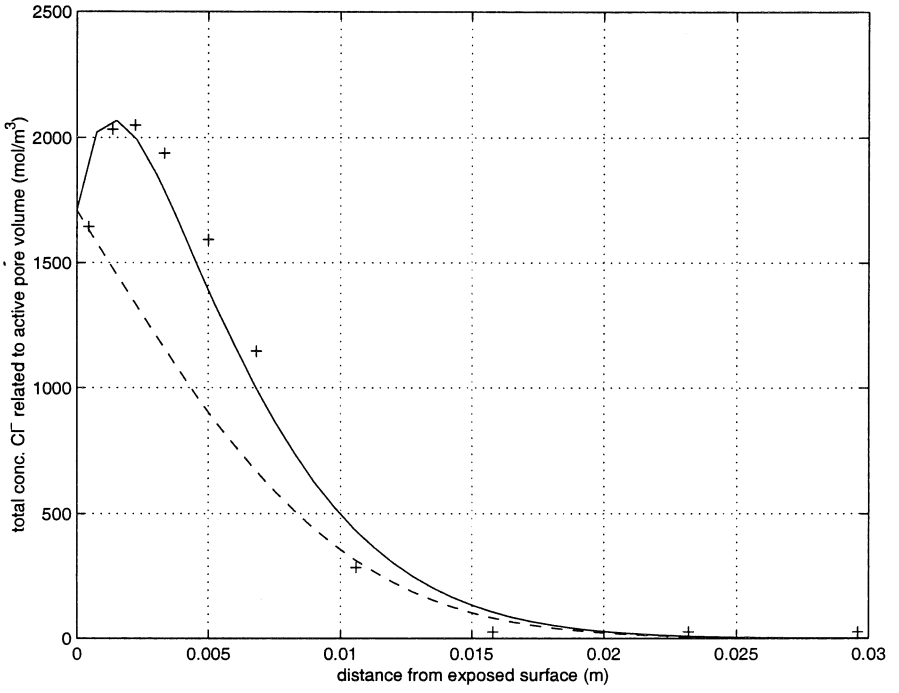

Figure 3: *SRPC concrete with 5% silica, water to binder ratio 0.40, exposed for 119 days to 3 wt.% sodium chloride solution. The concrete sample was dried for 14 days and rewetted for 7 days in tap water before being exposed to chlorides. The solid line represents simulated results for total chloride concentration as related to active water-filled volume. The dashed line is the simulated result when excluding dielectric effects. The plus signs represent measured values as related to active water-filled volume.*

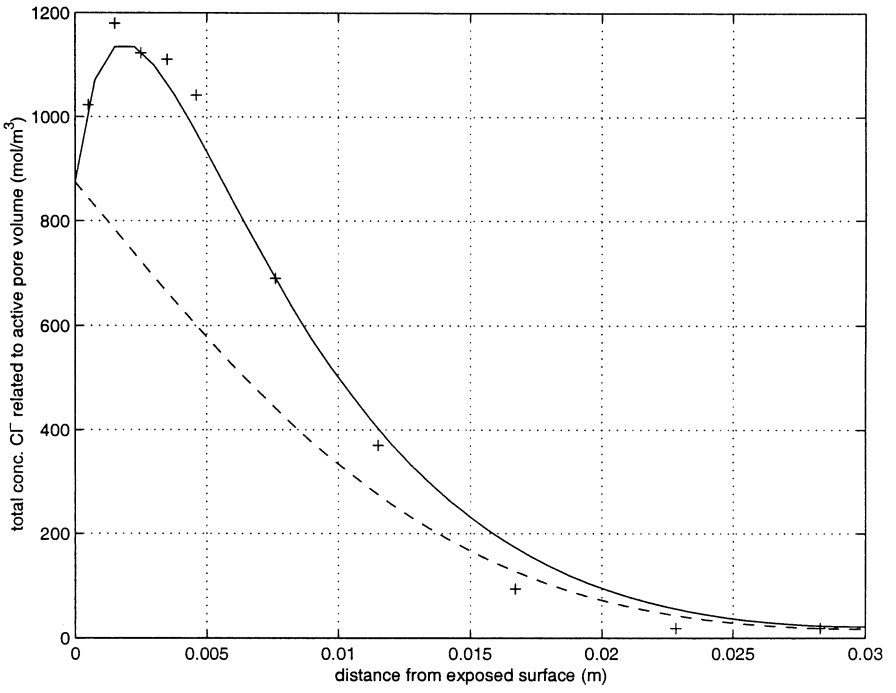

Figure 4: *SRPC concrete with 5% silica, water to binder ratio 0.55, exposed for 119 days to 3 wt.% sodium chloride solution. The concrete sample was dried for 14 days and rewetted for 7 days in tap water before being exposed to chlorides. The solid line represents simulated results for total chloride concentration as related to active water-filled volume. The dashed line is the simulated result when excluding dielectric effects. The plus signs represent measured values as related to active water-filled volume.*

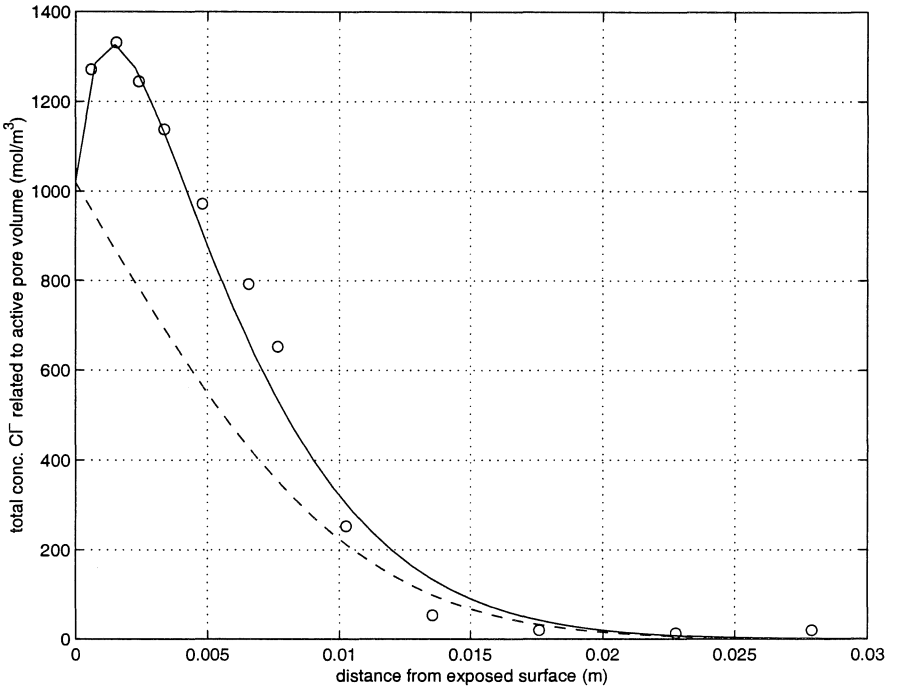

Figure 5: *SRPC concrete with 5% silica and 20% fly ash, water to binder ratio 0.40, exposed for 119 days to 3 wt.% sodium chloride solution. The concrete sample was dried for 14 days and rewetted for 7 days in tap water before being exposed to chlorides. The solid line represents simulated results for total chloride concentration as related to active water-filled volume. The dashed line is the simulated result when excluding dielectric effects. The circles represent measured values as related to active water-filled volume.*

are treated with separate constitutive relations not directly related to the diffusion. The change in porosity and in the shape of the pore system due to development of a higher degree of hydration during the chloride exposure tests is ignored. Therefore the obtained values for the tortuosity factor and binding capacities must be seen as mean values of the specific material tested being subjected to a certain pre-curing.

In all essential parts the simulations performed are done to obtain the best fit with the experimental data, by testing different values of the tortuosity factor and by specifying different values of the constants describing the equilibrium conditions and kinetics for binding of chlorides, i.e. K, Z and R, and leaching of hydroxide, i.e. W and Q. The dissolution of chlorides from already formed calcium chloride is assumed to be inactive in the studied experiments and the constant S is therefore set to zero. Further, the material constant Z is set to zero in the simulations performed, i.e. assuming that chloride binding is independent of hydroxide ion concentration in pore solution.

It was seen from several numerical tests runs that a quite good match between experimental data and simulations was obtained by using the same binding rate for all different concretes tested. Furthermore, only two different numbers were used for the constant describing the leaching rate for hydroxide in which a higher value was used for specimens dried for 14 days before exposure to chlorides. The binding capacity for the hydroxide ions in pore solutions was obtained by assuming that the initial state is an equilibrium condition, i.e. the value relating the initial mole concentration of hydroxide ions in pore solution to the mole concentration of solid calcium hydroxide in hydration products. For simplicity the initial value of the concentration of solid calcium hydroxide in concrete is assumed to be the same for all concrete qualities. It is realized, however, that an estimate of this concentration could be obtained by using the amount and composition of the cement in use in the different tested concretes.

A crucial point is to define an active porosity in which dissolved ions can appear. Depending on samples being dried or not before testing, either the measured active porosity or a calculated porosity is used. The values of porosities presented in Tables 15-17 are used. It should be noted that a certain adopted described value of active porosity will affect the value of binding capacity of chloride and hydroxide since the material constants describing the binding are related to the mole density concentration of ions in pore solution and not to the mass concentration of ions given per unit

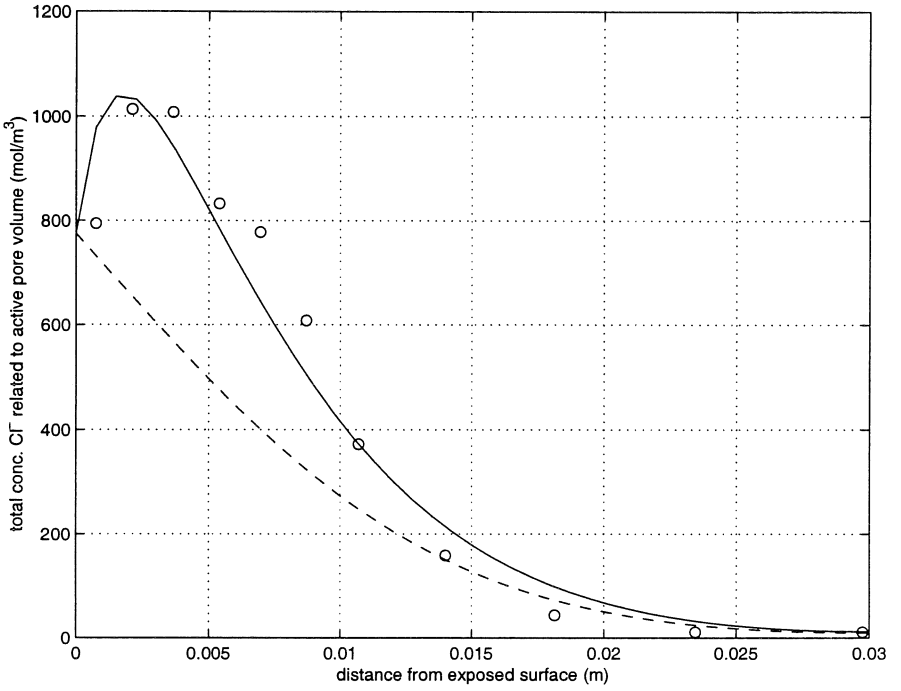

Figure 6: *SRPC concrete with 5% silica and 20% fly ash, water to binder ratio 0.55, exposed for 119 days to 3 wt.% sodium chloride solution. The concrete sample was dried for 14 days and rewetted for 7 days in tap water before being exposed to chlorides. The solid line represents simulated results for total chloride concentration as related to active water-filled volume. The dashed line is the simulated result when excluding dielectric effects. The circles represent measured values as related to active water-filled volume.*

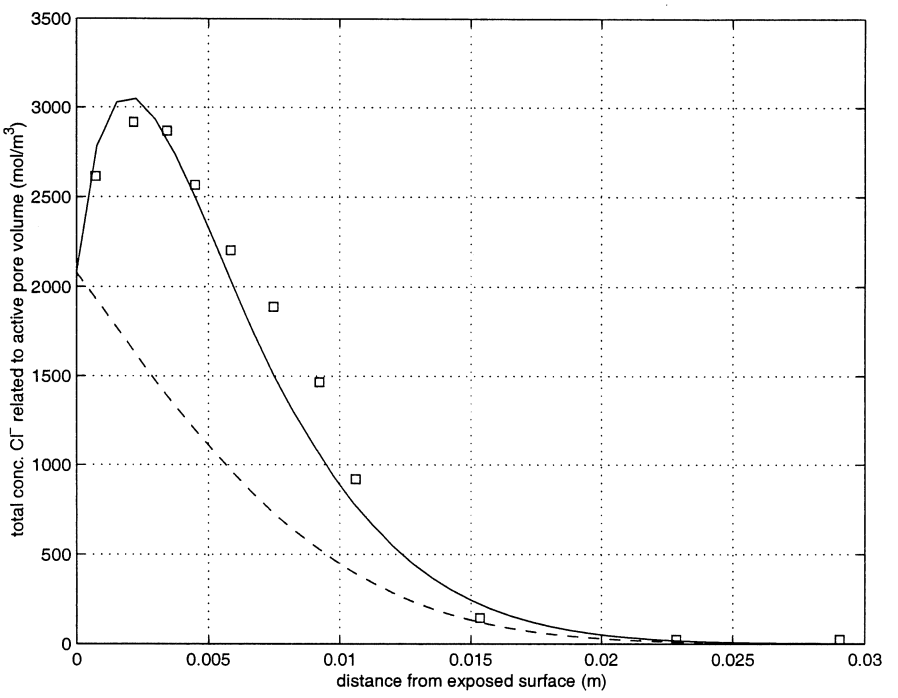

Figure 7: *OPC cement, water to cement ratio 0.40, exposed for 119 days to 3 wt.% sodium chloride solution. The concrete sample was dried for 14 days and rewetted for 7 days in tap water before being exposed to chlorides. The solid line represents simulated results for total chloride concentration as related to active water-filled volume. The dashed line is the simulated result when excluding dielectric effects. The squares represent measured values as related to active water-filled volume.*

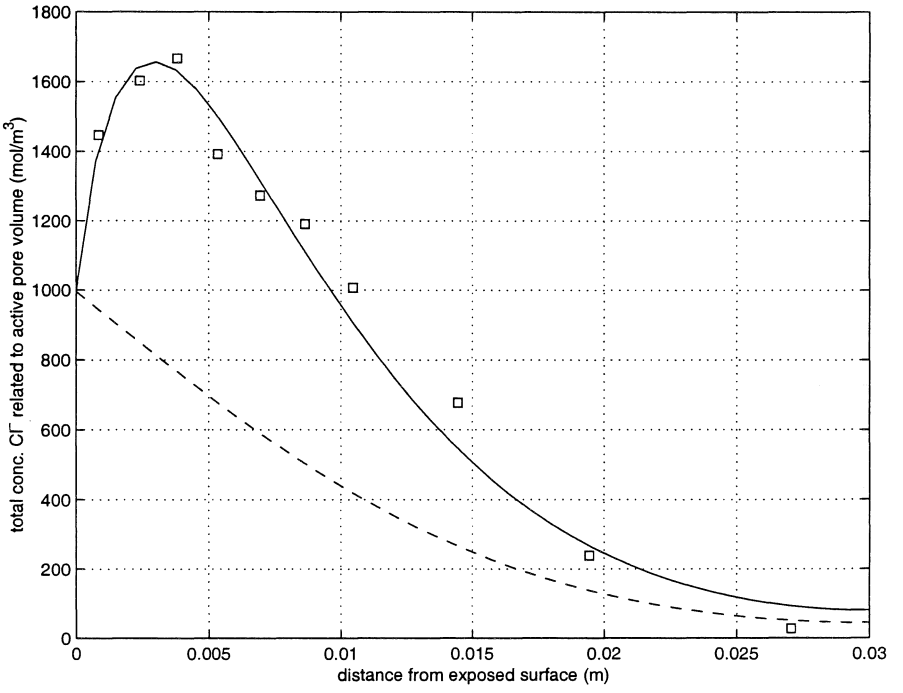

Figure 8: *OPC concrete, water to cement ratio 0.55, exposed for 119 days to 3 wt.% sodium chloride solution. The concrete sample was dried for 14 days and rewetted for 7 days in tap water before being exposed to chlorides. The solid line represents simulated results for total chloride concentration as related to active water-filled volume. The dashed line is the simulated result when excluding dielectric effects. The squares represent measured values as related to active water-filled volume.*

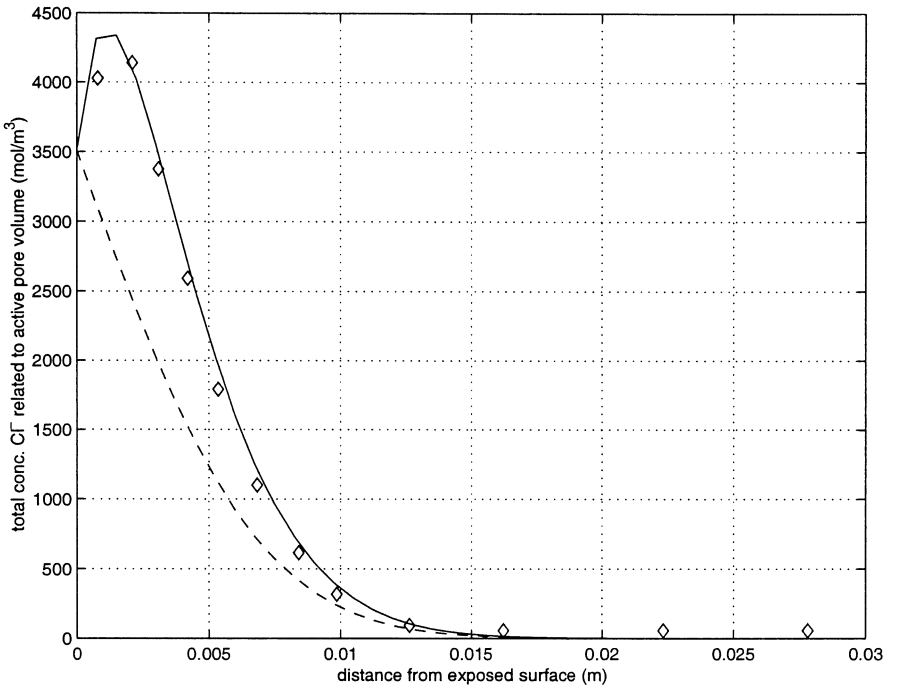

Figure 9: *OPC concrete with 5% silica, water to binder ratio 0.40, exposed for 119 days to 3 wt.% sodium chloride solution. The concrete sample was dried for 14 days and rewetted for 7 days in tap water before being exposed to chlorides. The solid line represents simulated results for total chloride concentration as related to active water filled volume. The dashed line is the simulated result when excluding dielectric effects. The diamonds represent measured values as related to active water-filled volume.*

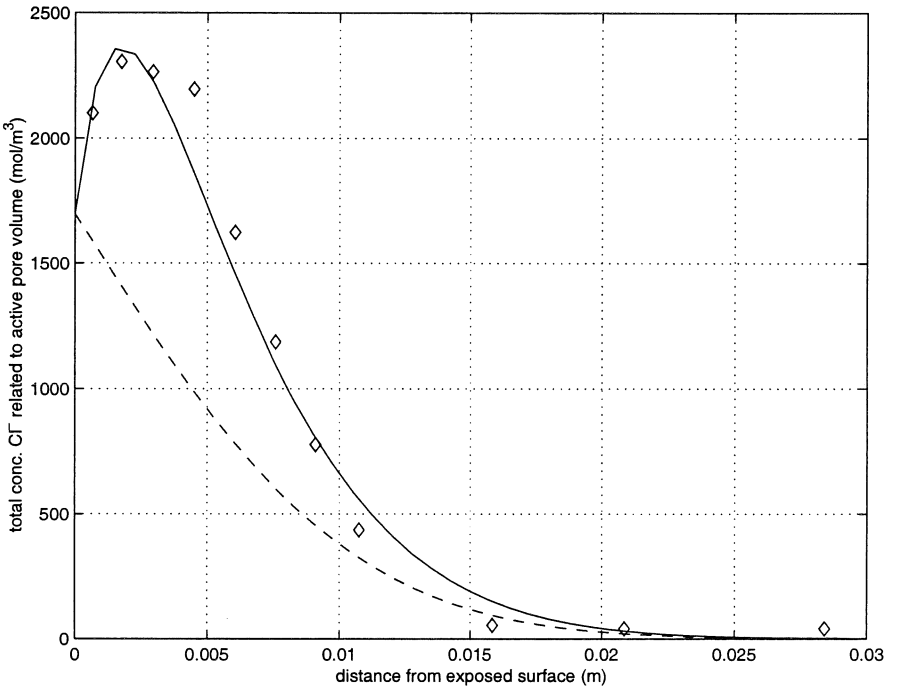

Figure 10: *OPC concrete with 5% silica, water to binder ratio 0.55, exposed for 119 days to 3 wt.% sodium chloride solution. The concrete sample was dried for 14 days and rewetted for 7 days in tap water before being exposed to chlorides. The solid line represents simulated results for total chloride concentration as related to active water-filled volume. The dashed line is the simulated result when excluding dielectric effects. The diamonds represent measured values as related to active water-filled volume.*

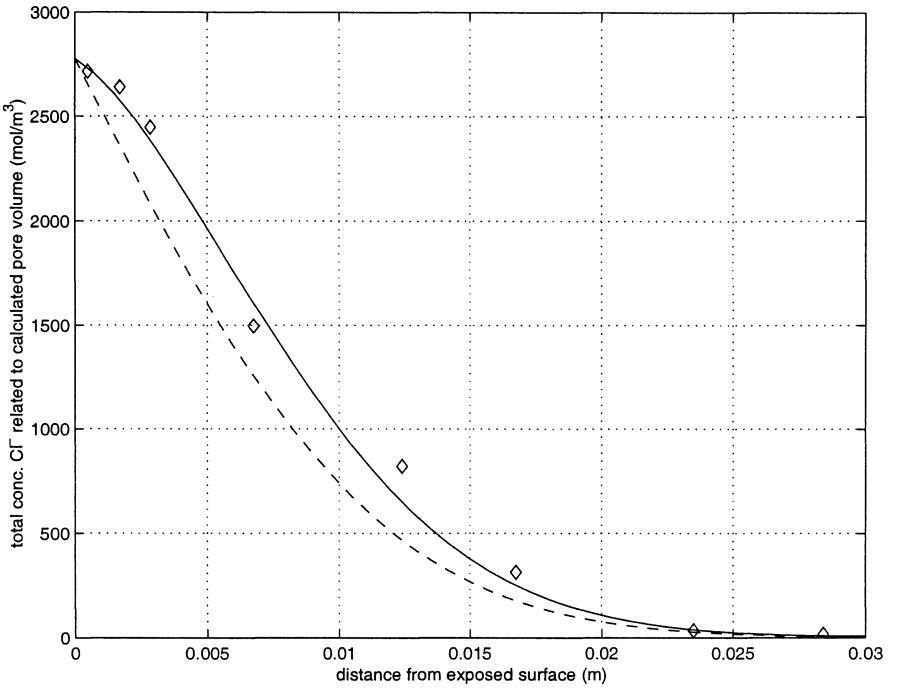

Figure 11: *SRPC concrete, water to cement ratio 0.40, exposed for 119 days to 3 wt.% sodium chloride solution. The sample was stored in tap water for 7 days before being exposed to chlorides. The solid line represents simulated results for total chloride concentration as related to the calculated active water-filled volume. The dashed line is the simulated result when excluding dielectric effects. The diamonds represent measured values as related to the calculated water-filled volume (total porosity).*

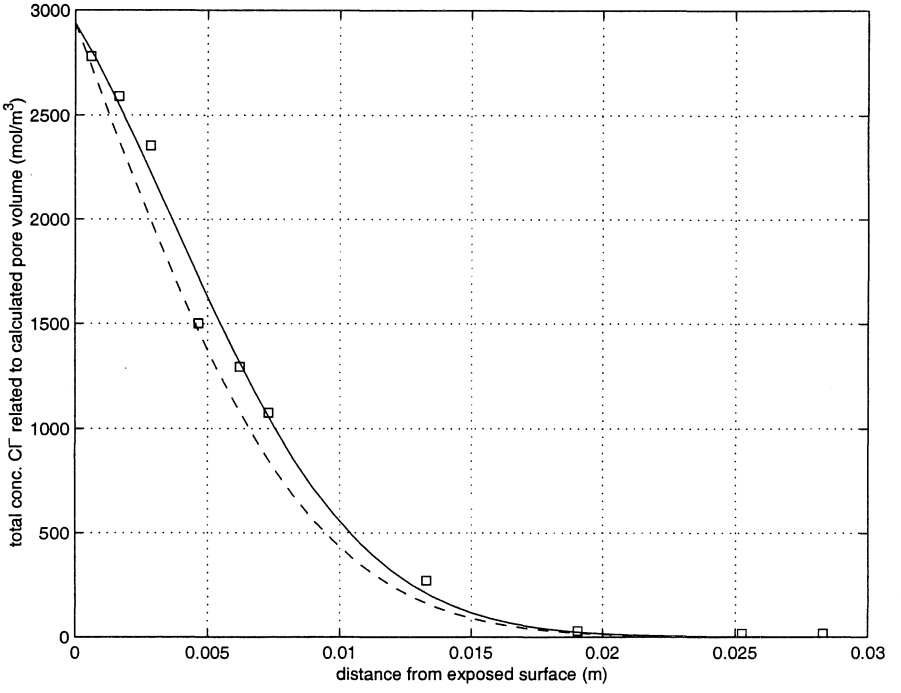

Figure 12: *SRPC concrete with 5% silica, water to binder ratio 0.40, exposed for 119 days to 3 wt.% sodium chloride solution. The sample was stored in tap water for 7 days before being exposed to chlorides. The solid line represents simulated results for total chloride concentration as related to the calculated active water-filled volume. The dashed line is the simulated result when excluding dielectric effects. The squares represent measured values as related to the calculated water-filled volume (total porosity).*

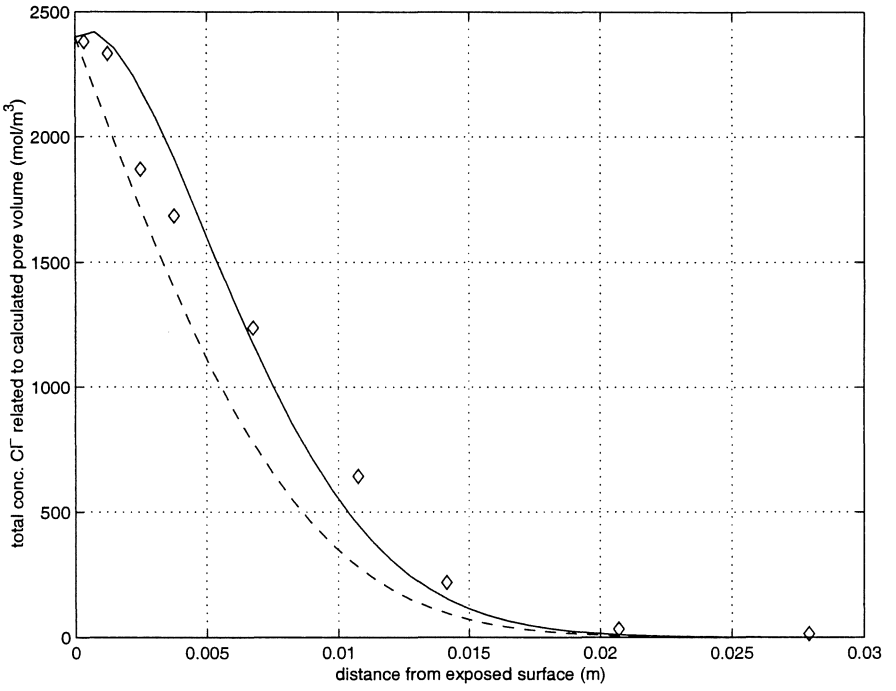

Figure 13: *OPC concrete, water to cement ratio 0.40, exposed for 119 days to 3 wt.% sodium chloride solution. The sample was stored in tap water for 7 days before being exposed to chlorides. The solid line represents simulated results for total chloride concentration as related to the calculated active water-filled volume. The dashed line is the simulated result when excluding dielectric effects. The diamonds represent measured values as related to the calculated water-filled volume (total porosity).*

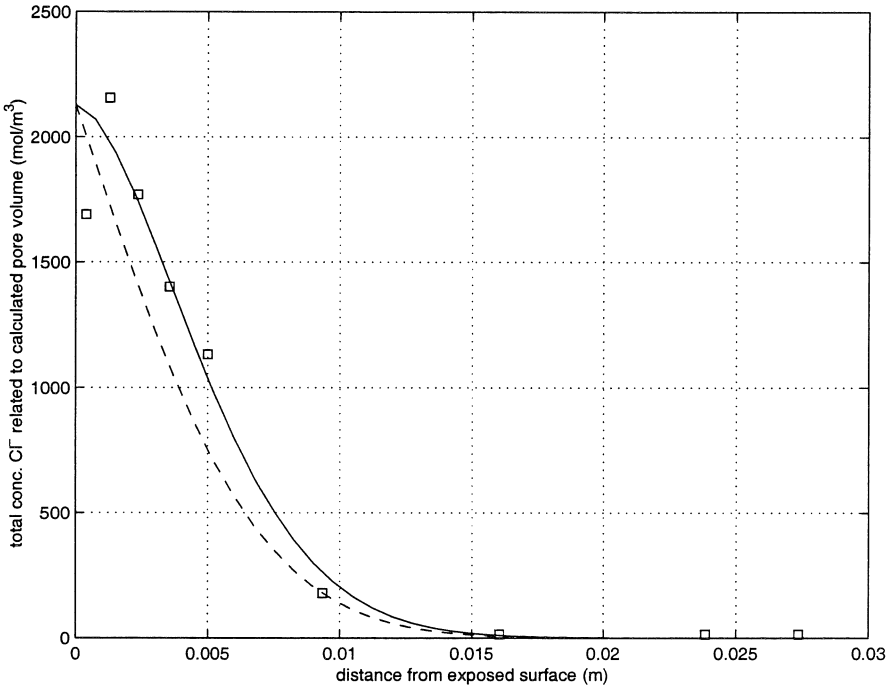

Figure 14: *OPC concrete with 5% silica, water to binder ratio 0.40, exposed for 119 days to 3 wt.% sodium chloride solution. The sample was stored in tap water for 7 days before being exposed to chlorides. The solid line represents simulated results for total chloride concentration as related to the calculated active water-filled volume. The dashed line is the simulated result when excluding dielectric effects. The squares represent measured values as related to the calculated water-filled volume (total porosity).*

Table 36: Results for SRPC concretes with no pozzolans. Specimens were dried for 14 days and rewetted for 7 days before exposure to chlorides.

Material constants	w/c 0.40	w/c 0.55
Tortuosity factor (-)	0.0115	0.0121
Binding cap., Cl^-, $1/K$ (-)	3.03	0.98
Binding rate, Cl^-, R (1/s)	0.0012	0.0012
Binding cap., OH^-, W (-)	0.0169	0.0169
Binding rate, OH^-, Q (1/s)	$1 \cdot 10^{-6}$	$1 \cdot 10^{-6}$
Measured active porosity	0.0691	0.1031

volume of the material as a whole.

Besides the conclusion drawn from the obtained tortuosity factor and binding capacity and kinetics of the reactions involving chlorides and hydroxide obtained by the simulations performed, two different evaluations have been performed. The first is a curve fitting of the measured results given as mass percent chlorides per mass concrete by using Fick's second law. This method is performed without any special attention to boundary conditions and binding of chlorides. The second approach of analyzing the measured chloride profiles is simply to check at which depth the concentration has reached 0.1 mass percent chlorides per mass concrete.

The results in terms of chloride profiles, as related to active water-filled pore volume (or to calculated water-filled total porosity), are presented for all tested concrete qualities based on pure cement or with addition of silica fume and fly ash. In order to compare measured values with simulation, the experimentally obtained total chloride content given as mass chlorides per mass concrete, has been recalculated to be valid as a concentration being smeared out in pore solution whose volume concentration, in material volume, corresponds to the active porosity. Further, the simulated total concentration of chlorides, as presented with solid lines in Figures 1-14, is obtained by summing the concentration field n_1 (free concentration of chloride ions in pore solution) and the concentration of n_6 (concentration of chloride ions involved in solid calcium chloride).

The results for pure SRPC concrete with the water to cement ratio 0.40 and 0.55 are presented in Figures 1 and 2. A better match between simulation and experiments was obtained for the 0.55 quality than for to the 0.40 ratio, when considering values near the exposed surface. The rather poor match for

Table 37: Results for SRPC concretes with 5 percent silica fume. Specimens were dried for 14 days and rewetted for 7 days before exposure to chlorides.

Material constants	w/b 0.40	w/b 0.55
Tortuosity factor (-)	0.0053	0.00561
Binding cap., Cl^-, $1/K$ (-)	1.18	0.36
Binding rate, Cl^-, R (1/s)	0.0012	0.0012
Binding cap., OH^-, W (-)	0.0103	0.0103
Binding rate, OH^-, Q (1/s)	$1 \cdot 10^{-6}$	$1 \cdot 10^{-6}$
Measured active porosity	0.0788	0.1070

Table 38: Results for SRPC concretes with 5 percent silica fume and 20 percent fly ash. Specimens were dried for 14 days and rewetted for 7 days before exposure to chlorides.

Material constants	w/b 0.40	w/b 0.55
Tortuosity factor (-)	0.0033	0.0055
Binding cap., Cl^-, $1/K$ (-)	0.50	0.26
Binding rate, Cl^-, R (1/s)	0.0012	0.0012
Binding cap., OH^-, W (-)	0.0111	0.0111
Binding rate, OH^-, Q (1/s)	$1 \cdot 10^{-6}$	$1 \cdot 10^{-6}$
Measured active porosity	0.1010	0.1213

the 0.40 is, among other things, due to having several properties constant for all studied concrete qualities. The solid lines represent the simulations when taking into account dielectric effects among ions which can be compared to the dashed lines, which is the result of a simulation when the electrostatic potential is set at zero in the whole domain, i.e. excluding dielectric effects. The difference between simulated values when taking into account dielectrical effects and when excluding this phenomenon, is shown to be greater for the 0.55 ratios than for the 0.40 ratios, e.g. compare Figure 1 and 2. The material coefficients used in the simulation for the two water to binder ratios are shown in Table 36. It is seen that the tortuosity factor for diffusion in pore system was lower and the binding capacity was higher for the 0.40 water to binder ratio than compared to the 0.55 ratio. This is a general result for all examined samples having different water to binder ratios.

The simulated profiles for SRPC concretes with 5% silica fume replacing

Table 39: Results for OPC concretes with no pozzolans. Specimens were dried for 14 days and rewetted for 7 days before exposure to chlorides.

Material constants	w/c 0.40	w/c 0.55
Tortuosity factor (-)	0.0066	0.0082
Binding cap., Cl^-, $1/K$ (-)	1.53	0.48
Binding rate, Cl^-, R (1/s)	0.0012	0.0012
Binding cap., OH^-, W (-)	0.0298	0.0298
Binding rate, OH^-, Q (1/s)	$1 \cdot 10^{-6}$	$1 \cdot 10^{-6}$
Measured active porosity	0.0561	0.0736

cement at the water to binder ratios 0.40 and 0.55 are presented in Figures 3 and 4. A good match between simulation and experimentally obtained values is obtained for both these qualities. It is also observed that when using the total concentration related to active pore volume, the concentration becomes greater for the lowest tested water to binder ratio, i.e. 0.40. This is due to a combined effect of having a greater capability of binding and a smaller active water-filled porosity for the tested 0.40 ratios compared to the 0.55 ratios. The adopted choices of material coefficient used for the two simulations of SRPC concretes with 5% silica fume are presented in Table 37.

The results for SRPC concretes with 5% silica fume and 20% fly ash are shown in Figure 5 (0.40 ratio) and Figure 6 (0.55 ratio). The concentration as related to active pore volume is shown to be significantly smaller than for SRPC concretes with 5% silica and concretes based on pure SRPC, compare Figures 3 and 4 with Figures 1-4. In [27] and [28] strong evidence suggests that the degree of chloride binding in concrete decreases when silica fume is used in mix. One possible explanation is that it lowers the CaO/SiO_2 ratio, and this effect can be expected to dominate the binding process. In this investigation it was found that the chloride binding capacity for plain SRPC concrete is reduced by a factor of 3 when replacing 5 wt.% of the cement by silica fume, i.e. compare Tables 36 and 37. On the other hand the tortuosity factor for plain SRPC concrete is reduced by a factor of 2 when using 5 wt.% silica fume replacing cement, see Table 36 and 37. The overall performance, expressed in terms of the effective chloride diffusion which includes effects caused by both chloride binding and diffusion in the pore system of concrete, reveals that inclusion of silica fume reduces the penetration of chlorides, i.e. the decrease in chloride binding is compensated by the decreased tortuosity

Table 40: Results for OPC concretes with 5 percent silica fume. Specimens were dried for 14 days and rewetted for 7 days before exposure to chlorides.

Material constants	w/b 0.40	w/b 0.55
Tortuosity factor (-)	0.0050	0.0056
Binding cap., Cl^-, $1/K$ (-)	2.94	1.16
Binding rate, Cl^-, R (1/s)	0.0012	0.0012
Binding cap., OH^-, W (-)	0.0200	0.0200
Binding rate, OH^-, Q (1/s)	$1 \cdot 10^{-6}$	$1 \cdot 10^{-6}$
Measured active porosity	0.0365	0.0491

for diffusion of chlorides, see Tables 45 and 46.

The chloride profiles and simulations for OPC concretes are shown in Figures 7-10. A satisfying agreement was obtained for all these different tests. The OPC concrete with 5% silica, see Figure 9, showed the lowest ingress of chlorides of all examined samples. The chloride binding capacity for the blended OPC concrete was found to be less affected by silica fume than the blended SRPC concrete. Inclusion of 5 wt.% silica resulted in an increase of binding capacity by a factor of 2 compared to plain OPC concrete and the tortuosity factor was reduced by about 30%, see Tables 39 and 40. The increase of binding capacity when using silica fume together with OPC is contradictory to other reported results, e.g. see [27] and [28]. It should be noted, however, that the active porosity was observed to be unaffected by inclusion of silica fume when used together with SRPC; when comparing the measured active porosity for plain OPC concrete and OPC concrete with 5% silica fume it is concluded that the latter had about 40% smaller active porosity. This will affect the values of the binding capacities as the concentration of free diffusing chlorides is related to the water-filled active porosity.

Comparing plain OPC and SRPC concretes, it is concluded that the OPC-based samples have about twice as low tortuosity factors than the SRPC-based samples, on the other hand the SRPC concretes have a factor 2 larger binding capacity, see Tables 36 and 39. Therefore the effective diffusion of chlorides in plain OPC and SRPC concretes differs very little, see Table 43.

The set of samples stored for 7 days in tap water before exposure, whose experimental and simulated results are presented in Figures 11-14, showed fewer effects caused by dielectrics compared to samples dried for 14 days

Table 41: Results for OPC and SRCP concretes, with no pozzolans, cured in water for 7 days before exposure to chlorides.

Material constants	SRPC, w/c 0.40	OPC, w/c 0.40
Tortuosity factor (-)	0.0110	0.0055
Binding cap., Cl^-, $1/K$ (-)	2.22	1.85
Binding rate, Cl^-, R (1/s)	0.0012	0.0012
Binding cap., OH^-, W (-)	0.0169	0.0298
Binding rate, OH^-, Q (1/s)	$2 \cdot 10^{-7}$	$2 \cdot 10^{-7}$
Calculated porosity	0.1177	0.1426

followed by rewetting for 7 days in tap water before exposure, the results of which are shown in Figures 1-10. The comparable small difference between dashed lines (dielectric effects excluded) and solid lines in Figures 11-14, compared to the results in Figures 1-10, confirms this condition. In order to match the experimentally obtained values to the model, for samples never dried before exposure, the dissolution rate of hydroxide ions from solid product was forced to be significantly smaller than for samples dried for 14 days before exposure, see Tables 36-42.

The dependence of the binding capacity of chlorides and the tortuosity factor for chloride diffusion on cement type and pozzolans differed significantly depending on whether the samples were dried before exposure or not. This is presumably caused by the fact that the water-filled total porosity used as important data to calculate the binding capacity and tortuosity factors, for samples never dried before exposure, are incorrect. That is, the calculated porosities are very little affected by inclusion of silica fume and the type of cement used. This behavior is not found on the measured active porosities for samples dried before exposure, e.g. compare the porosities used in Tables 36, 37, 39 and 40 with the ones in Tables 41 and 42.

In order to compare the results obtained from fitting the material constants in the governed equations described in section 3 to the traditional method leading to the effective diffusion constant, D_{eff}, for chloride penetration into concrete, an effective diffusion constant, denoted D^*_{eff}, will be calculated. This value is formed as: $D^*_{eff} = \tilde{D}_1 / (1 + 2K^{-1})$, in which $\tilde{D}_1$ is the scaled bulk diffusion coefficient for chlorides dissolved in pore solution and K^{-1} can be referred to as the binding capacity of chlorides in pore system of concrete. The relation $D^*_{eff} = \tilde{D}_1 / (1 + 2K^{-1})$ can be derived for

Table 42: Results for OPC and SRCP concretes with 5 percent silica fume cured in water for 7 days before exposure to chlorides

Material constants	SRPC, w/b 0.40 5% silica	OPC, w/b 0.40 5% silica
Tortuosity factor (-)	0.00682	0.00302
Binding cap., Cl^-, $1/K$ (-)	2.38	1.59
Binding rate, Cl^-, R (1/s)	0.0012	0.0012
Binding cap., OH^-, W (-)	0.0103	0.0200
Binding rate, OH^-, Q (1/s)	$-2 \cdot 10^{-7}$	$-2 \cdot 10^{-7}$
Calculated porosity	0.1179	0.1370t

a simple system of two constituents where only one constituent is allowed to have a diffusion velocity different from zero. Consider a diffusion equation, given as $\partial \rho_{cl}/\partial t = \tilde{D}_1 \partial^2 \rho_{cl}/\partial x^2 - \partial \rho_{cl}^b/\partial t$, where $-\partial \rho_{cl}^b/\partial t$ is the mass exchange rate between dissolved chlorides in pore solution and bound chlorides. The equilibrium binding isotherm relation is assumed to be given as: $\rho_{cl}^b = 2K^{-1}\rho_{cl}$, where ρ_{cl}^b and ρ_{cl} denote the mass density concentration of bound chlorides and chlorides appearing as dissolved in pore solution, respectively. The relation $\rho_{cl}^b = 2K^{-1}\rho_{cl}$ together with the above diffusion equation yields $\partial \rho_{cl}/\partial t = \tilde{D}_1/\left(1 + 2K^{-1}\right) \partial^2 \rho_{cl}/\partial x^2$. This relation is obtained, simply, by eliminating ρ_{cl}^b by using the assumed binding isotherm. It is seen that the effective diffusion coefficient, defined as $D_{eff}^* = \tilde{D}_1/\left(1 + 2K^{-1}\right)$, is the term replacing the normal diffusion constant in the derived equation. The equilibrium binding isotherm $\rho_{cl}^b = 2K^{-1}\rho_{cl}$ corresponds to the equilibrium condition used in the model described in section 3, when setting $Z = 0$, i.e. $n_1^{eq} = Kn_6$. The multiple two used in $\rho_{cl}^b = 2K^{-1}\rho_{cl}$ is due to this relation being expressed in terms of mass density concentrations and the relation $n_1^{eq} = Kn_6$ in mole density concentrations.

When using the effective diffusion constant, which includes chloride binding, it must be assumed that a one-to-one relation (for linear or non-linear binding isotherms) always exists between bound and dissolved chloride ions in pore solution. This means that the binding must be instantaneous, i.e. the equilibrium condition given from the binding isotherm must be reached instantaneously when the concentration of chlorides is changed due to diffusion. The kinetics of the reaction, as included in the model described in section 3, can therefore not be included when establishing a model based on

Table 43: Comparision of two different calculated effective chloride diffusion constants. The specimens were dried for 14 days and rewetted for 7 days before exposure to chlorides.

Concrete types	D^*_{eff} (m^2/s)	D_{eff} (m^2/s)
SRPC, w/c 0.40	$3.32 \cdot 10^{-12}$	$4.31 \cdot 10^{-12}$
SRPC, 5% silica, w/b 0.40	$3.20 \cdot 10^{-12}$	$1.73 \cdot 10^{-12}$
SRPC, 5% silica 20% fly ash, w/b 0.40	$3.35 \cdot 10^{-12}$	$2.60 \cdot 10^{-12}$
OPC, w/c 0.40	$3.29 \cdot 10^{-12}$	$3.69 \cdot 10^{-12}$
OPC, 5% silica, w/b 0.40	$1.46 \cdot 10^{-12}$	$1.22 \cdot 10^{-12}$
SRPC ,w/c 0.55	$8.30 \cdot 10^{-12}$	$7.20 \cdot 10^{-12}$
SRPC, 5% silica, w/b 0.55	$6.64 \cdot 10^{-12}$	$3.68 \cdot 10^{-12}$
SRPC, 5% silica 20% fly ash, w/b 0.55	$7.35 \cdot 10^{-12}$	$3.26 \cdot 10^{-12}$
OPC, w/c 0.55	$8.58 \cdot 10^{-12}$	$7.90 \cdot 10^{-12}$
OPC, 5% silica, w/b 0.55	$3.42 \cdot 10^{-12}$	$2.12 \cdot 10^{-12}$

the effective diffusion constant.

The obtain values for D^*_{eff} and D_{eff} are shown in Table 43, in which the results for specimens dried for 14 days followed by rewetting in tap water before exposure are presented. The results for the samples subjected to 7 day's storage in tap water before exposure are shown in Table 44. A greater difference between D^*_{eff} and D_{eff} values is obtained for the case presented in Table 43 compared to the values in Table 44. This is, mainly, due to ignoring the experimentally obtained values near the exposed surface when calculating the value D_{eff}.

The depths at which the chloride content is 0.1 (weight percent by concrete mass), are calculated by linear interpolation on the measured profiles presented in Tables 20-33. The interpolated depths at which the chloride content is 0.1 are shown in Tables 45 and 46. The highest penetration depth of the examined qualities was obtained for the SPRC with no pozzolans and with the water to cement ratio 0.55, 16.1 mm, and the lowest value was obtained for the OPC concrete with 5% silica replacing cement, 5.2 mm.

Table 44: Comparison of two different calculated effective chloride diffusion constants. The specimens were cured in tap water for 7 days before exposure to chlorides.

Concrete types	D^*_{eff} (m^2/s)	D_{eff} (m^2/s)
SRPC, w/c 0.40	$4.10 \cdot 10^{-12}$	$5.23 \cdot 10^{-12}$
SRPC, 5% silica, w/b 0.40	$2.40 \cdot 10^{-12}$	$2.78 \cdot 10^{-12}$
OPC, w/c 0.40	$2.38 \cdot 10^{-12}$	$3.63 \cdot 10^{-12}$
OPC, 5% silica, w/b 0.40	$1.47 \cdot 10^{-12}$	$1.55 \cdot 10^{-12}$

Table 45: Comparison between concrete qualities. The depth at which the chloride concentration is 0.1 weight percent by concrete mass for samples dried for 14 days and stored in tap water for 7 days before exposure at 119 days.

Concrete types	$d_{0.1}$ (mm)
SRPC, w/c 0.40	11.8
SRPC, 5% silica, w/b 0.40	8.0
SRPC, 5% silica 20% fly ash, w/b 0.40	7.5
OPC, w/c 0.40	9.9
OPC, 5% silica, w/b 0.40	5.2
SRPC, w/c 0.55	16.1
SRPC, 5% silica, w/b 0.55	8.3
SRPC, 5% silica 20% fly ash, w/b 0.55	9.2
OPC, w/c 0.55	11.6
OPC, 5% silica, w/b 0.55	7.0

Table 46: Comparison between concrete qualities. The depth at which the chloride concentration is 0.1 weight percent by concrete mass. The specimens were cured in tap water for 7 days before exposure to chlorides at 119 days.

Concrete types	$d_{0.1}$ (mm)
SRPC, w/c 0.40	14.5
SRPC, 5% silica, w/b 0.40	11.0
OPC, w/c 0.40	12.1
OPC, 5% silica, w/b 0.40	7.9

5 Conclusions

For the studied OPC concrete with and without 5% silica, SRPC concrete with and without 5% silica and SRPC with 5% silica and 20% fly ash replacing cement, the OPC with 5% silica had the slowest ingress of chlorides for both studied pre-curing conditions before exposure. All three methods of evaluating the measured data gave this result. The two different studied preparations, after one day of membrane hardening were: drying in room climate for 14 days followed by rewetting in tap water for 7 days, and curing in tap water for 7 days before exposure to chlorides.

The measured active porosity on the concretes based on pure SRPC was slightly smaller than compared to concretes based on SRPC with 5% silica replacing cement. The active porosity for the pure SRPC-based concretes was significantly lower than for concretes where 5% silica and 20% fly ash replaced the SRPC in mix. For OPC-based concretes the active porosity was found to be significantly lower when 5% of cement was replaced with silica compared with a pure OPC concrete with the same water to binder ratio. Porosity estimations based on the cement content and the measured hydration degree did not, in general, reflect the behavior detected by measuring the active porosity by capillary suction experiments.

When using the definition of the active volume in which dissolved ions can appear given from the measured active porosity, it was found that replacement of 5% OPC by silica resulted in a lower tortuosity factor and a higher binding capacity of chlorides when compared to a concrete based on pure OPC. However, when using the calculated porosity for samples never dried before exposure to chlorides, it was found that the binding capacity

of chlorides was very little affected by inclusion of 5% silica replacing cement compared to pure cement, whereas the tortuosity factor was decreased significantly when using silica.

The tortuosity factor increases as the active porosity and the calculated porosity increases for the concretes based on the same cement and pozzolans but with different water to binder ratios. No general dependency between porosity and the tortuosity factor could be found for the different concrete qualities containing different cements and pozzolans. This indicates that the tortuosity depends not only on the porosity but also on the shape of the pore system. That is, two different concrete mixes based on different cements and pozzolans having the same active porosity can have very different shape of the pore system, therefore resulting in different tortuosity factors.

The relation between the binding capacity of chlorides and the cement content follows the same pattern as the relation between tortuosity and porosity, i.e. for the same type of cement and pozzolan based concrete with different water to binder ratios the binding capacity of chlorides decreases with decreased cement content. The important difference obtained when comparing all types of different compositions, with respect to chloride binding capacity, is presumably caused by different specific surfaces and chemical composition of solid components in contact with the pore solution.

The difference between the evaluated measures D^*_{eff} and D_{eff} was observed to be most dominant for samples stored for 7 days in tap water before exposed to chlorides, compared to samples being dried before exposure. This observation was independent of the type of cement and pozzolans in use. The reason for obtaining significantly different values of D^*_{eff} and D_{eff} for the case of samples dried for 14 days and rewetted in tap water for 7 days before exposure is that the experimentally obtained concentration of chlorides near the exposed surface is ignored when estimating D_{eff}, since these points do not match the solution of Fick's second law. The proposed model as described in section 3 does not suffer from drawbacks of this kind.

Even though better results were obtained, from the performed experiments, in terms of resistance of chloride ingress in OPC-based concretes compared to SRPC-based concretes, the general conclusion concerning which cements to be used in a saline environment is not straightforward. One important issue, among others, is that concretes based on OPC suffer a high risk of being subjected to sulfate attack in environments where SO_4^{2-} is present.

The method of having different equations describe the diffusion of ions in pore solution and chemical binding has several benefits. First of all, the

dielectric effects can be modeled. Furthermore, the suggested approach is developed in a way which opens up for the possibility to model other phenomena than those described in this work. For example, the effect of convection of ions in pore solution due to capillary suction, influence of temperature on ion diffusion, binding and dissolution can be incorporated, without changing the main underlying assumptions and definitions.

Several experimental tests must, however, be performed to verify the model in its current state. The most important issue is, perhaps, to measure the concentration profiles of other ions than chlorides, since all types of ions are essential due to the dielectric effects included in the model. Another type of experiment is to check the development of concentration profiles over time. In this study, the measured chloride profiles were only fitted against the model at one time level only.

References

[1] Sharif, A.A., Loughlin K.F. Azad, A.K. and Navaz, C.M. (1997). *Determination of the Effective Chloride Diffusion Coefficient in Concrete via a Gas Diffusion Technique*, ACI Materials Journal, Vol. 94, No. 3, pp. 227-233.

[2] Martys, N.S. (1999). *Diffusion in Partially-Saturated Porous Materials.* Materials and Structures, Vol. 32, pp. 555-562.

[3] Samson, E., Marchand, J. and Beaudoin, J.J. (1999). *Describing ion diffusion mechanisms in cement-based materials using the homogenization technique.* Cement and Concrete Research, Vol. 29, pp. 1341-1345.

[4] Glass, G.K., Hassanein, N.M. and Buenfeld, N.R. (1997). *Neural Network Modelling of Chloride Binding.* Magazine of Concrete Research, Vol. 49, No. 181, pp. 323-335.

[5] Haque, M.N. and Kayyali O.A. (1995). *Aspects of Chloride Ion Determination in Concrete*, ACI Materials Journal, Vol. 92, No. 5, pp. 532-541.

[6] Wee, T.H., Wong, S.F., Swaddiwudhipong, S. and Lee, S.L. (1997). *A Prediction Method for Long-Term Chloride Concentration Profiles in Hardening Cement Matrix Materials.* ACI Materials Journal, Vol. 94, No. 6, pp. 565-579.

[7] Dhir, R.K., Hewlett, P.C. and Dyer, T.D. (1999). *Chemical Profiles of Cement Pastes Exposed to a Chloride Solution Spray*, Cement and Concrete Research, Vol. 29, pp. 667-672.

[8] Page, C.L., Short, N.R. and El Tarras A. (1981). *Diffusion of Chloride Ions in Hardened Cement Pastes.* Cement and Concrete Research, Vol. 11, pp. 395-406.

[9] Mangat, P.S. and Molloy, B.T. (1995). *Chloride Binding in Concrete Containing PFA, gbs or Silica Fume under Sea Water Exposure*, Cement and Concrete Research, Vol. 47, No. 171, pp. 129-141.

[10] Page, C.L, Short, N.R. and Holden, W.R. (1986). *The Influence of Different Cements on Chloride-induced Corrosion of Reinforcing Steel*, Cement and Concrete Research, Vol. 16, pp. 79-86.

[11] Shiqun, Li and Della M. Roy (1986). *Investigation of Relations Between Porosity, Pore Structure, and* Cl^- *Diffusion of Fly Ash and Blended Cement Pastes*, Cement and Concrete Research, Vol. 16, pp. 749-759.

[12] Chan S.Y.N and Ji X. (1999). *Comparative Study of the Initial Surface Adsorption and Chloride Diffusion of High Performance Zeolite, Silica Fume and PFA Concretes*, Cement & Concrete Composites Vol. 21. pp. 293-300.

[13] Alexander M.G. and Magee B.J. (1999). *Durability Performance of Concrete Containing Condensed Silica Fume*, Cement and Concrete Research, Vol. 29, pp. 917-922.

[14] Thomas M.D.A and Bamforth P.B. (1999). *Modelling Chloride Diffusion in Concrete Effect of Fly Ash and Slag*, Cement and Concrete Research, Vol. 29, pp. 487-495.

[15] *Chloride Penetration into Concrete*, Proceedings of the International Workshop St. Rémy-lès-Chevreuse, France, 15-18 October 1995, Edited by Lars Olof Nilsson and Jean-Pierre Ollivier (RILEM Publications, France).

[16] *Corrosion of Reinforcement, Field and Laboratory Studies for Modelling and Service Life*, Proceedings of the Nordic Seminar in Lund, Sweden,

1-2 February 1995, Edited by Kyösti Tuutti, Division of Building Technology, Lund University of Technology.

[17] Janz, J and Johannesson, B.F. (1993). *A Study of Chloride Penetration into Concrete* (in Swedish), Division of Building Technology, Lund University of Technology.

[18] Nagesh, M. and Bishwajit B. (1998). *Modelling of Chloride Diffusion in Concrete and Determination of Diffusion Coefficients*, ACI Materials Journal, Vol. 95, No. 2, pp. 113-120.

[19] Tang, L. (1999). *Concentration Dependence of Diffusion and Migration of Chloride Ions, Part 1. Theoretical Considerations*, Cement and Concrete Research, Vol. 29, pp. 1463-1468.

[20] Tang, L. (1999). *Concentration Dependence of Diffusion and Migration of Chloride Ions, Part 2. Theoretical Considerations*, Cement and Concrete Research, Vol. 29, pp. 1469-1474.

[21] Costa, A. and Appleton, J. (1999). *Chloride Penetration into Concrete in Marine Environment - Part 1: Main Parameters Affecting Chloride Penetration*, Materials and Structures, Vol. 32, pp. 252-259.

[22] Weast, R.C., Lide, D.R. Astle, M.J. and Beyer, W.H. (1989). *Handbook of Chemistry and Physics*, 70^{TH} edition, CRC Press, Inc. Boca Raton, Florida.

[23] Atkins, P.W. (1994). *Physical Chemistry*, Fifth Edition, Oxford University Press, Oxford.

[24] Zienkiewicz, O.C. and Taylor, R.L. (1989). *The Finite Element Method,* Fourth Edition, Vol. 2, McGraw-Hill, London.

[25] Bathe, K.J. (1996). *The Finite Element Procedures*, Prentice Hall, Englewood Cliffs, New Jersy.

[26] Hughes, T.J.R. (1987). *The Finite Element Method, Linear Static and Dynamic Finite Element Analysis,* Prentice-Hall International Editions.

[27] Page, C.L. and Vennesland, O. (1983). *Pore Solution Composition and Chloride Binding Capacity of Silica-fume Cement Pastes*, Materials and Structures, Vol. 16, No. 91. pp. 19-25.

[28] Rasheeduzzafar, S., Hussain, S.E. and Al-Gahtani, A.S. (1991). *Pore Solution Composition and Reinforcement Corrosion Characteristics of Microsilica Blended Cement Concrete.* Cement and Concrete Research, Vol. 21, no. 6, pp. 1035-1048.

LUNDS TEKNISKA
HÖGSKOLA
Lunds universitet